Analysis

The distribution of subsurface microplastics in the ocean

https://doi.org/10.1038/s41586-025-08818-1

Received: 28 September 2023

Accepted: 20 February 2025

Published online: 30 April 2025

Open access

Check for updates

Shiye Zhao[1]✉, Karin F. Kvale[2], Lixin Zhu[3,4], Erik R. Zettler[5], Matthias Egger[6,7], Tracy J. Mincer[8], Linda A. Amaral-Zettler[5,9], Laurent Lebreton[6], Helge Niemann[5,10], Ryota Nakajima[1], Martin Thiel[11,12,13], Ryan P. Bos[14], Luisa Galgani[15,16] & Aron Stubbins[4,17,18]

Marine plastic pollution is a global issue, with microplastics (1 µm–5 mm) dominating the measured plastic count[1,2]. Although microplastics can be found throughout the oceanic water column[3,4], most studies collect microplastics from surface waters (less than about 50-cm depth) using net tows[5]. Consequently, our understanding of the microplastics distribution across ocean depths is more limited. Here we synthesize depth-profile data from 1,885 stations collected between 2014 and 2024 to provide insights into the distribution and potential transport mechanisms of subsurface (below about 50-cm depth, which is not usually sampled by traditional practices[3,6]) microplastics throughout the oceanic water column. We find that the abundances of microplastics range from 10^{-4} to 10^{4} particles per cubic metre. Microplastic size affects their distribution; the abundance of small microplastics (1 µm to 100 µm) decreases gradually with depth, indicating a more even distribution and longer lifespan in the water column compared with larger microplastics (100 µm to 5,000 µm) that tend to concentrate at the stratified layers. Mid-gyre accumulation zones extend into the subsurface ocean but are concentrated in the top 100 m and predominantly consist of larger microplastics. Our analysis suggests that microplastics constitute a measurable fraction of the total particulate organic carbon, increasing from 0.1% at 30 m to 5% at 2,000 m. Although our study establishes a global benchmark, our findings underscore that the lack of standardization creates substantial uncertainties, making it challenging to advance our comprehension of the distribution of microplastics and its impact on the oceanic environment.

Marine plastic pollution is a global issue[7], with 9–14 million metric tons of plastics entering the ocean annually[8]. Microplastics (1 µm–5 mm)[1] dominate measured plastic counts and pose serious global threats to ocean health[9,10]. Most studies focus on surface waters, collecting microplastics from the upper 15–50 cm using net tows[5]. However, microplastics exist in various forms with complex properties that affect their interactions with the environment[11,12] (Box 1), ultimately shaping their three-dimensional distribution[13]. Consequently, microplastics are found throughout the water column, from the coastal to open ocean, across all latitudes[3,4,14–16]. Despite this, a synthesis of current knowledge and research priorities regarding microplastics across ocean depths is lacking.

The water column of the ocean, providing the most voluminous habitat on Earth, has a vital role in biogeochemical cycling[17]. The ocean contributes approximately 50% of global net primary production, serves as a major sink for anthropogenic carbon dioxide[18], and facilitates particle transport and distribution[17,19]. As marine particles and microplastics transit the water column, their interactions with biogeochemical processes influence their behaviour and impact marine ecosystems[17,19,20], including the ocean's carbon cycle[21,22]. Therefore, understanding the distribution and potential impacts of microplastics throughout the water column is essential.

To advance understanding of the distribution of microplastics, here we synthesize depth-profile data from 1,885 stations collected between 2014 and 2024 (Fig. 1a), describing distribution patterns by size and polymer type, and assessing potential transport mechanisms. We examine existing microplastics distribution models and highlight research challenges and priorities (Table 1) for advancing knowledge of subsurface microplastics distributions and impacts in the ocean.

[1]Japan Agency for Marine-Earth Science and Technology, Yokosuka, Japan. [2]Aotearoa Blue Ocean Research, Lower Hutt, New Zealand. [3]State Key Laboratory of Estuarine and Coastal Research, East China Normal University, Shanghai, China. [4]Department of Marine and Environmental Sciences, Northeastern University, Boston, MA, USA. [5]NIOZ Royal Netherlands Institute for Sea Research, Den Burg, The Netherlands. [6]The Ocean Cleanup, Rotterdam, The Netherlands. [7]Empaqtify, St Gallen, Switzerland. [8]Harriet Wilkes Honors College, Florida Atlantic University, Boca Raton, FL, USA. [9]Department of Freshwater and Marine Ecology, Institute for Biodiversity and Ecosystem Dynamics, University of Amsterdam, Amsterdam, The Netherlands. [10]Department of Earth Sciences, Faculty of Geosciences, Utrecht University, Utrecht, The Netherlands. [11]Facultad Ciencias del Mar, Universidad Catolica del Norte, Coquimbo, Chile. [12]MarineGEO Program, Smithsonian Environmental Research Center, Edgewater, MD, USA. [13]Centre for Ecology and Sustainable Management of Oceanic Island (ESMOI), Coquimbo, Chile. [14]Department of Organismic and Evolutionary Biology, Harvard University, Cambridge, MA, USA. [15]Department of Biotechnology, Chemistry and Pharmacy, University of Siena, Siena, Italy. [16]National Biodiversity Future Center (NBFC), Palermo, Italy. [17]Department of Chemistry and Chemical Biology, Northeastern University, Boston, MA, USA. [18]Department of Civil and Environmental Engineering, Northeastern University, Boston, MA, USA. ✉e-mail: szhao@jamstec.go.jp

Box 1

Complexity of microplastics in the natural environment

Microplastics (1 µm to 5 mm)[1] constitute a complex suite of contaminants with a wide array of physicochemical and biological characteristics, including size, shape, density, colour, chemistry and biofilm composition[12]. These diverse properties arise from both plastic manufacturing processes and natural transformations. The chemical composition and structure of microplastics determine fundamental traits such as material type, shape, size, density and resistance to environmental stressors such as heat and ultraviolet radiation[11]. In addition, plastic additives further modulate these properties[133].

In natural environments, secondary microplastics are generated through the fragmentation of larger plastic debris and undergo various physical (for example, sunlight, heat, wind and waves) and biological (for example, fragmentation via biting, ingestion and biofouling) transformations[11], increasing their diversity. This complexity greatly complicates sampling and analysing techniques (Extended Data Table 1), creating challenges in comparing or synthesizing microplastic data across different studies. Field studies typically classify microplastics into discrete categories (see the figure). Size, shape and density are key factors influencing the transport and fate of environmental microplastics. Furthermore, characteristics such as colour, surface properties, eco-toxin sorption and additives influence the ecological risk posed by microplastics. Biologically, microplastics host diverse microbial communities, including non-native species, potential pathogens and antibiotic-resistant genes, forming what is referred to as the 'plastisphere'[41].

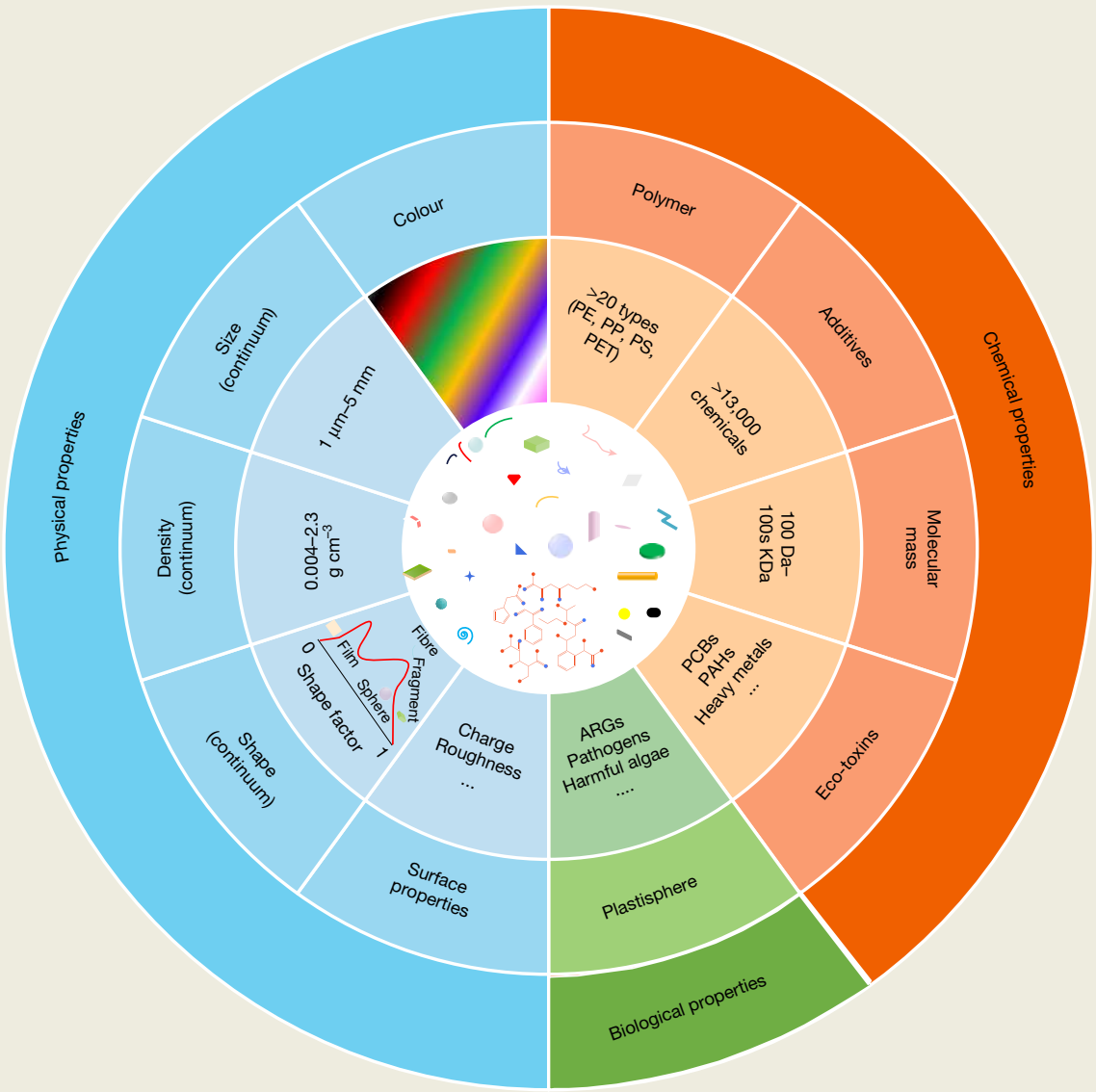

Box 1 Fig. 1 | Complexity of microplastics in the natural environment. Microplastics vary in physical (size, shape, density, surface properties), chemical (polymer type, additives, molecular structure, adsorbed chemicals), and biological (plastic-associated microbiome, the 'plastisphere') properties. These factors, shaped by manufacturing and environmental influences, complicate the measurements of microplastics and influence their ecological impact. ARGs, antibiotic-resistant genes; PAHs, polycyclic aromatic hydrocarbons; PCBs, polychlorinated biphenyls; PE, polyethylene; PP, polypropylene; PS, polystyrene; PET, polyethylene terephthalate.

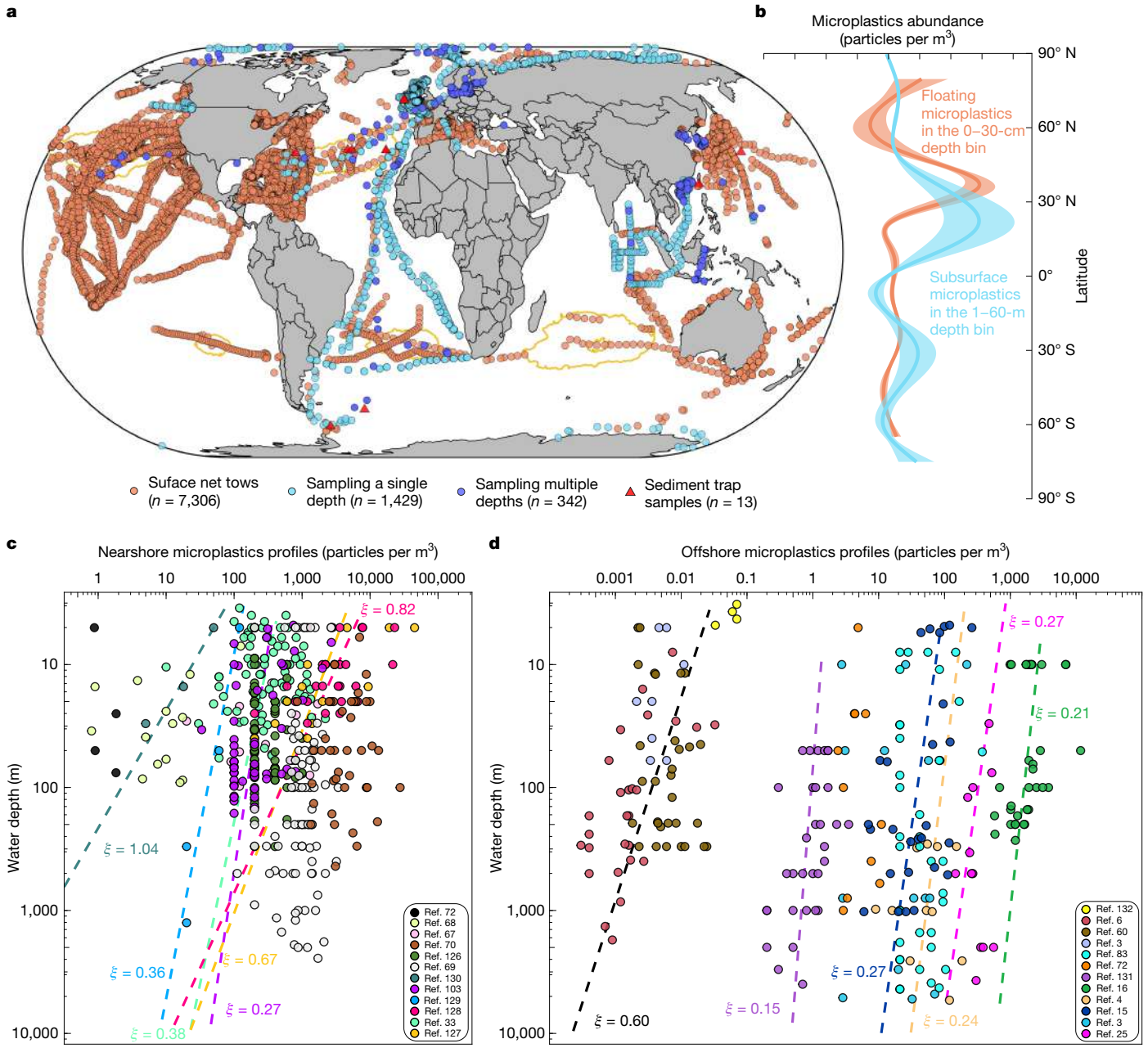

Fig. 1 | Observations of subsurface microplastics in the ocean. a, Global observation stations of marine microplastics collected through surface net tows (orange dots; data from refs. 2,5,89,124), at a single depth beneath the surface using various techniques (light blue dots), from multiple water depths (dark blue dots), and from sediment traps (red triangles). The solid yellow lines represent the predicted boundaries of the offshore convergence zones, where floating plastic debris accumulates[125]. **b**, Latitudinal trends in the adjusted large microplastics, residing within the 1–60-m depth bin (light blue line, subsurface microplastic data collected at a single depth in refs. 55,77–86) and those floating microplastics at the sea surface (0–50 cm, orange line; data from ref. 5). Only the trends of coloured lines are considered here (for exact values, refer to Supplementary Fig. 1). The coloured shaded areas denote ±1 s.d. from 1,000 Monte Carlo runs that used varying predictors for the Generalized Additive Models (GAMs). **c**,**d**, Depth profiles of microplastic abundances (particles per m^3) observed in nearshore (**c**; data from refs. 33,67–70,72,103,126–130) and offshore (**d**; data from refs. 3,4,6,15,16,25,60,72,83,131,132) waters with the log–log regression fits (dashed lines) between microplastics abundances and water depth of individual studies. The exponent (ξ), also referred to as the slope, provides information on the rate of abundance change along the depth gradients. The lower particle size limit of each study in **c** and **d** is presented in Supplementary Table 3. The corresponding linear regression equations are shown in Supplementary Table 4.

Uncertainties in microplastic measurement methods

The reported abundance of water column microplastics spans eight orders of magnitude (Supplementary Table 1). It needs to be noted that some of this variation arises from inconsistencies in collection and analysis methods (Extended Data Table 1 and Supplementary Tables 2 and 3). The physicochemical and biological characteristics of aged microplastics further complicate measurements (Box 1), as each plastic category demands customized sampling and analysis approaches[23]. For instance, the use of 19 different pore sizes of meshes and filters (Supplementary Table 3) may contribute to pronounced differences in reported abundances; smaller pore sizes capture more particles, as microplastics counts typically increase with decreasing size, following an approximate power law[24]. This effect is evident in parallel sampling efforts, where samples collected at the same site and depth but using 10-µm versus 500-µm meshes yielded

Table 1 | Current understanding, process insights and research priorities for subsurface microplastics

Current knowledge and confidence level	Process insights	Major gaps and priority level
Distribution Spatial distribution: • Microplastics permeating throughout the water column (H) • Higher abundances in nearshore than offshore waters (M) • Abundances of large microplastics decline sharply with depth[24,35,60] (H) • An even distribution of small microplastics[12,14,23] (H) • Subsurface maximum occurring in the bathypelagic layer[10–12] (H) • Plastic-C:POC ratio increase with depth[20,23] (L) Size distribution: • Microplastics under 100 µm dominate the count[11,12,14,23] (H) • Nanoparticles were confirmed[121] (L) Polymer distribution: • Buoyant polymers dominating overall (L) • Dense polymers being more prevalent offshore and in deeper waters (M) • Specific polymers differing between nearshore and offshore (M) Shape category/distribution: • Non-fibrous particles and fibre (M) **Mechanisms** Physically mediated processes: • Wind-driven mixing transports microplastics downwards[122] (H) • Eddy subduction delivers small microplastics to depth[35,36] (L) • Water stratification retains large microplastics[11,56] (M) • Slow currents converge microplastics[10,11] (L) Biologically mediated processes: • Biofilm alone can rarely sink microplastics to the sea floor[42,46] (H) • Microplastics flux with a power-law profile is confirmed[20] (L) • Faecal pellets and mineral ballast are an efficient shuttle to export microplastics to the deep sea[34,43,123] (L)	• Proximity to terrestrial sources, shallow water depth and high biological activities may contribute to high concentrations in nearshore waters • As particles get smaller, size largely determines their transport and fate • Small microplastics, regardless of their densities, sink at comparable speeds • The non-degradable plastic-C is changing the marine C system, especially in the deep sea • Variations in the degradation potential of polymers and different plastic sources may contribute to spatial differences in polymer distribution • Particle retention time in stratified layers increases quadratically with particle size[73] • Seasonal stratification may pump large microplastics into deeper depths • Marine aggregates are an important vector to transport microplastics to the deeper waters[20]	**Enhancing standardization and data resolution:** • Standardize protocols (H) • Coordinated abundance observations on regional and global scales (M) • Long-time monitoring of microplastics flux from nearshore to offshore in different biogeochemical provinces (H) • Leverage archived marine particle samples (M) • Enhance nanoplastic and microfibre observation (H) • Develop continuous, high-resolution monitoring techniques (M) • Constrain the boundary of microplastics accumulation zones beneath the surface (M) **Improving particle characterization:** • Define size, shape, density, colour and chemical signature following a continuous distribution (H) • Estimate in situ density of microplastics, including plastic and any biotic/abiotic materials on its surface (M) • Advance methods for quantifying plastic ages and carbon composition (M) **Addressing microplastics source:** • Explore the exchange between the ocean and the atmosphere (H) • Better understand plastic fragmentation in both nearshore and offshore waters (M) **Defining key parameters of biological and physical transport mechanisms:** • Study the physical structure of microplastics-associated biofilm, such as thickness, roughness, cell number and biomass (L) • Estimate sinking rates of environmentally relevant microplastics colonized by biofilm, incorporated into marine snow and faecal pellets (H) • Quantify the effects of biogenic minerals on the vertical flux of plastics (H) • Study the changes in microbiome of plastic-laden marine snow during their transit through the water column (L) • Explore transport efficiency of physical subduction such as seasonal variations of water stratification and eddies (M) **Model optimization:** • Developing environmentally relevant microplastic parameterizations based on experiments and observations, specifically focusing on plastic-C:organic-C ratios in particle fluxes, particle sinking rates, remineralization rates and zooplankton ingestion rates (H) • Creation of standardized datasets from which to assess model performance (H) • Improved mechanistic parameterizations of the biotic and abiotic fragmentation of plastics (H) • Improved estimates of sources and sinks to constrain the global microplastics budget (H)

This table provides a structured assessment of the current state of knowledge on subsurface microplastics, summarizing key insights into their behaviour and associated processes. It includes an overview of current understanding, a qualitative ranking (high (H), medium (M) or low (L)) of how well each topic is understood, major unresolved questions and critical research gaps. In addition, it assigns priority levels (high (H), medium (M) or low (L)) for future investigations over the coming years.

5–6 orders of magnitude differences in microplastic abundances[6,25]. Analytical techniques also drive discrepancies. Microscopy-aided preselection followed by chemical identification—a method applied in 70% of studies—relies heavily on the investigators' experience and becomes unreliable for small microplastics[26]. For instance, a study employing micro-Fourier transform infrared (µ-FTIR) imaging, capable of identifying polymers particles down to 11 µm (ref. 27), revealed 2–3 orders of magnitude more microplastics in Arctic sea-ice cores than earlier light-microscopy-based estimates[28]. Variability may also result from subsampling rather than analysing the entire sample. Extrapolating results from subsamples can introduce biases of up to +600% (refs. 29,30). These methodological uncertainties currently hinder accurate quantification of the distribution of microplastics in the environment. Research efforts aimed at enhancing observation resolution in the water column, while employing consistent methods, are crucial in refining our understanding of the marine microplastics standing stock, whether measured by count or by mass.

Microplastics permeating ocean waters

Our synthesis reveals that subsurface microplastics sampling is concentrated in the Atlantic and Atlantic–Arctic oceans (Fig. 1a). In waters between 1 m and 60 m, large microplastics abundances, determined at a single depth and represented by light blue dots in Fig. 1a, can reach up to 800 particles per m^3 (ref. 31), with a median of 0.49 particles per m^3 (Extended Data Fig. 1). Comparing microplastic abundances in comparable size fractions (>200 µm; Methods), reveals consistent latitudinal patterns between subsurface microplastics (1–60 m) and floating microplastics (median: 0.02 particles per m^3; upper 0.5 m; ref. 6), both peaking in subtropical zones (Fig. 1b). However, subsurface microplastic counts at 1–60 m depth are approximately significantly higher than those at the surface ($P < 0.05$, Extended Data Fig. 1).

Despite uncertainties, measurements from studies collecting samples at multiple depths per station (median 205 particles per m^3; range 10^{-4} to 10^4 particles per m^3, represented by dark blue dots in Fig. 1a) suggest that the water column represents a major reservoir of

microplastics. High abundances have been consistently observed in deep waters, including over 1,100 particles per m^3 at 100–270 m in a North–South Atlantic transect[16], 600 particles per m^3 at 2,000 m in the North Pacific Subtropical Gyre[25], 200 particles per m^3 at 2,500 m in the Arctic[4], and 13,500 particles per m^3 at 6,800 m in the Mariana Trench[32]. Along the Korean coast alone, an estimated 3.13 trillion microplastics sized 0.33–4.75 mm are present in the water column[33]. This accounts for a small but notable fraction of the 171 trillion floating plastics in the same size range observed globally, most of which are microplastics[2]. In the Atlantic Ocean, microplastics of the 32–651-µm size category in the top 200 m average 2,200 particles per m^3, with an estimated mass of 11.6–21.1 million metric tons. This mass is comparable to the total input of plastic in the >300-µm size category (17–47 million metric tons) into Atlantic waters and sediments from 1950–2015 estimated in ref. 16. However, these estimates are subject to substantial uncertainty owing to coarse observation resolution, simplified ocean physics and methodological inconsistencies.

Subsurface microplastic distribution patterns

Sampling locations were categorized as 'nearshore' (within 200 nautical miles from shore) and 'offshore' (beyond 200 nautical miles)[31]. Microplastic abundances ranged from 10^{-3} to 10^{4} particles per m^3 nearshore and from 10^{-4} to 10^{4} particles per m^3 offshore. Despite potential underestimation in nearshore studies using microscopy-aided methods, the median nearshore abundance (500 particles per m^3) is over 30 times higher than the median offshore abundance (16 particles per m^3) where advanced methods were often used (Supplementary Tables 2 and 3). This nearshore median aligns with values from offshore plastic accumulation zones confirmed via µ-FTIR imaging (for example, 400 particles per m^3 in the North Pacific Subtropical Gyre[25] and 250 particles per m^3 in the South Atlantic Subtropical Gyre[3]). High nearshore abundances match previous predictions and field observations[34–36], suggesting that coastal regions may act as plastic accumulation zones akin to offshore gyres[37]. Factors such as proximity to terrestrial sources[38] and shallow nearshore waters where turbulence draws plastics downwards[32,36] likely contribute to this observation.

Microplastic abundances generally decrease with water depth (Fig. 1c,d). Nearshore waters show a much steeper decrease in abundance compared with offshore waters ($P = 0.029$; Extended Data Fig. 2 and Supplementary Table 4), with abundances declining by up to a 1,000-fold (Fig. 1c). This sharp decline probably results from the high mineral and biological productivity in coastal waters, which enhances the sinking rates of aggregated microplastics[39]. Diatoms, dominant in coastal ecosystems, contribute siliceous frustules (density 2.6 g cm^{-3}) frequently found on the surface of microplastics, thereby increasing their ballast effect[40–42]. Similarly, calcite precipitates (density >2.63 g cm^{-3}) associated with biofouled microplastics add weight, accelerating their sinking[43]. Together, these factors promote efficient vertical transport of microplastics in nearshore waters. These findings agree with models predicting rapid sinking of microplastics in biological productive coastal zones with strong downwelling, such as in East Asia[34–36]. Conversely, low productivity in offshore waters may cause less efficient vertical transport[44–46], contributing to the observed differences in abundance decay rates. In addition, owing to its proximity to coastal plastic sources, the dilution effects on microplastic levels (stemming from coastal and riverine inputs) in coastal waters[38] could also cause this rapid concentration decline. Direct measurements of microplastic vertical flux are scarce and methodological variations hinder clear insights[22,47–53] (Supplementary Table 5). Future research should explore vertical transport mechanisms in ecosystems with varying biological productivity, combining concentration measurements with flux-profile analysis to improve understanding of the processes that transfer microplastics downwards, analogous to the study of particulate organic carbon[54].

Abundance profiles of offshore microplastics smaller than 100 µm show a gradual decrease (within one order of magnitude) with depth (Fig. 1d), implying a relatively even distribution throughout the water column[3,55,56]. Models also suggest a uniform dispersion of small microplastics (1–100 µm) in the water column, behaving differently from large microparticles[35,55,56], with sinking speeds ranging from 10^{-3} m s^{-1} to 10^{-6} m s^{-1}, regardless of buoyant[57] or dense[58,59] plastics. Even biofouling minimally alters the settling velocities of small microplastics owing to their restricted surface area[42]. A two-orders-of-magnitude decrease in the abundance of large microplastics (100 µm to 5,000 µm) with depth in offshore waters also supports this size-dependent distribution[6,60] (Fig. 1d). Models and observations show that, compared with small microplastics, large microplastics tend to either remain at the sea surface or quickly reach the sea floor, leading to a rapid decline in abundances along depth gradients[25,35,61].

Long-term observations are crucial to understanding microplastic abundance profiles and vertical fluxes. Capturing both discrete (such as polymers and colour) and continuous (such as size, shape and density) characteristics of microplastics is essential to elucidate physical and biological redistribution mechanisms[24,62]. Physical processes, such as seasonal stratification and eddy-driven subduction, differ in temporal and spatial scales[13] and remain poorly understood. Biological factors, such as the physical structure (for example, thickness, biomass and density[63,64]) of microplastic-attached biofilms across depths have rarely been studied. How microplastics interact with marine aggregates (composed of microbes, organic and inorganic matter[19]) during their transit through the water column, including factors such as sinking velocities and the cohesive strength of plastic-laden aggregates, also warrants future research.

Results are generally reported as counts, so measurements of the microplastic mass in the water column are limited. Microplastic mass concentrations vary by up to five orders of magnitude (Extended Data Fig. 3), partially attributed to methodological differences. In the North Pacific Subtropical Gyre, small and large microplastics concurrently sampled have comparable mass concentrations at shallow depths[6,25] (Extended Data Fig. 3), but the ratio of small to large microplastic mass increases with depth[25], highlighting the growing significance of small microplastics at greater depths.

Density stratification retaining large microplastics

Vertical density stratification in the ocean, driven by temperature and/or salinity gradients, creates pycnoclines, where the water density changes sharply[65]. These pycnoclines are common in the ocean and are often associated with intense biological activities and elevated concentrations of particles, such as the accumulation of marine snow[66]. Observations in both nearshore[56,67–71] and offshore waters[3,72] show increased microplastics within pycnocline layers compared with those above. Our synthesis suggests that the elevated abundances in stratified layers are mostly linked to large microplastics rather than small microplastics[3,33,56] (Fig. 2a). Stratification affects particle settling through a combination of buoyancy, diffusion and viscosity, which slows sinking by increasing drag and suppressing vertical motion, directing particles along isopycnals[73,74]. Whether stratification impacts a particle's motion depends on the stratification length scale (L), the distance over which water density changes, which ranges from 100 µm to 1 mm. Particles larger than L, such as large microplastics, are significantly affected, whereas smaller microplastics are largely unaffected[73]. Irregular-shaped particles undergoing stratification-induced reorientation experience further deceleration[75]. As a result, large and irregular microplastics experience prolonged settling times and concentrate at pycnoclines. The lack of small microplastic accumulation at density interfaces was also observed in a freshwater system[76]. Our findings also agree with a model study that identifies a pronounced accumulation of large microplastics at pycnoclines, compared with small microplastics, in the open

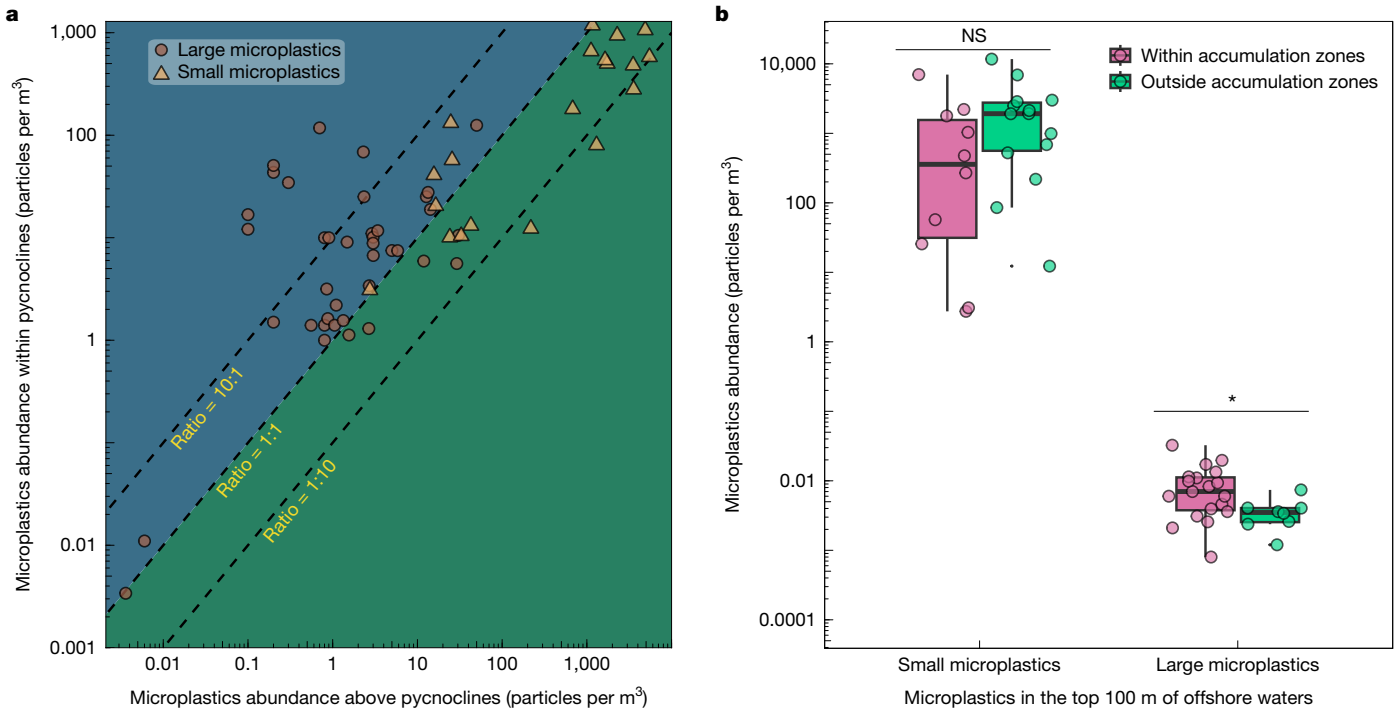

Fig. 2 | Vertical distribution of microplastics along water-depth gradients as a function of particle size, density stratification and sampling location. **a**, Relationship between microplastic abundance within pycnocline layers and those above the pycnocline layers as a function of microplastics size category: small microplastics (gold triangles; refs. 3,33,56) and large microplastics (brown dots; refs. 3,56,67–72). Dashed lines represent ratios of microplastic abundances within pycnocline layers to those above the pycnocline layers. Refer to Methods for large and small microplastics classification. **b**, Box-and-whisker plots for the measured abundances of small and large microplastics within and outside the well-known accumulation zones in the top 100 m of the water column (Methods). The datasets are from refs. 3,6,16,25,60, which sampled microplastics at multiple depths at each station (represented by dark blue dots in Fig. 1a). Bold black horizontal lines within the coloured boxes represent the boxplot medians, while the top and bottom of the boxes indicate the 25th and 75th percentiles. The whiskers indicate the largest and smallest measured values within 1.5 interquartile ranges from the box. The asterisk indicates a statistically significant difference between small microplastics and large microplastics ($P = 0.03$). 'NS' indicates no difference ($P = 0.11$).

ocean[46]. Further investigation into microplastics in pycnoclines and other distinct layers, such as the deep chlorophyll maximum and benthic nepheloid layers, is essential to understand not only transport but also the potential exposure of marine life.

Vertical extension of microplastic accumulation zones

Large microplastics, both floating at the sea surface (0–50-cm depth) and present in subsurface waters (data from refs. 55,77–86 collected at a single depth between 1 m and 60 m), peak in abundances at mid-latitudes (generalized additive models (GAMs), $P \ll 0.01$; Fig. 1b and Extended Data Fig. 1). However, their distribution varies along the latitudinal gradients. Elevated abundances are also observed in the 1–60-m depth range above 55° N and 60° S. The increased abundances at high latitudes align with modelling results, suggesting that subsurface currents carry microplastics to the polar regions[87]. Observations indicate that the Atlantic is the largest source of subsurface microplastics collected in Arctic waters[86]. Besides the input by oceanic flows, other sources such as atmospheric delivery and rivers (for example, Eurasian river inflows[15,86]) from lower latitudes[88] could also contribute to the pronounced microplastic abundances at high northern latitudes.

The accumulation of large microplastics at 1–60-m depths at mid-latitudes matches plastic convergence zones observed by surface net tows[89–91] and global models[92–94], suggesting that these zones extend deeper. Three-dimensional simulations of microplastic transport in the global ocean also affirms the persistence of subtropical microplastic convergence zones at certain water depths, showing that the structure of these accumulation zones in the gyres remains discernible down to 16 m and disappears at 60 m (ref. 87). Other models suggest that buoyant microplastics in the top 10 m of the water column follow the surface pattern, with high concentrations in mid-ocean gyres[35]. Our analysis of large microplastics measured at multiple depths at each station in the subtropical gyres also supports this finding. Within the top 100 m, large microplastic abundances in accumulation zones are significantly higher than outside ($P = 0.03$; Fig. 2b). However, this difference is not found below 100 m (Extended Data Fig. 4). The existence of large microplastic patches in the near-surface waters can be mainly explained by a combination of wind-driven Ekman currents and prolonged residence of large microplastics in the upper water column[35,95]. Taken together, accumulation zones of large microplastics extend into the oceanic water column, primarily constrained to the near-surface waters; a pattern not evident with small microplastics. Further research efforts are essential to constrain the subsurface boundaries of accumulation zones, characterize microplastics in each layer and assess their ecological impacts.

Plastic-carbon entering marine particulate carbon pool

Plastic debris represents a source of allochthonous carbon (C) to marine ecosystems. Subsurface microplastic-C has been estimated by calculating particle mass and multiplying it by the C% in the chemical formulas of common polymers[22,25]. Our analysis shows that the ratio of microplastic-C to total particulate organic carbon (POC) increases with depth in subtropical gyres ($P = 0.002$; Extended Data Fig. 5). This is because 75% of particulate organic matter is remineralized in the upper 500 m (ref. 96), compared with persistent plastic-C. The microplastic-C:POC ratio can reach up to 5% at 2,000 m, reflecting shifts in the overall particulate composition. With the increasing plastic

leakage into the ocean, substantial long-term addition of microplastic-C to the marine POC pool is anticipated. Microplastic-C, utilized by marine microbes alongside metabolites and organic debris released by microbial processes[97,98], can influence biogeochemical cycles, such as nitrification and denitrification[98]. However, plastic-C altering the marine POC pool has received little attention, necessitating further exploration, as marine POC is central to long-timescale carbon sequestration and biogeochemical cycling[19]. In addition, ^{14}C-depleted plastic-C can interfere with ^{14}C-based age determinations by reducing the fraction of radioactive ^{14}C (ref. 99). A 5% contribution of plastic-C could make marine POC samples appear approximately 420 years older than their true apparent age. Plastic-C introduces additional complexity to the interpretation of already scarce deep-ocean ^{14}C data, complicating our understanding of ocean circulation, carbon cycling and past climate conditions[100]. This calls for more plastic-C data and adjustments to models that predict or interpret deep-ocean ^{14}C levels.

A comparison of models with observations

Simulations increasingly explore the transport and fate of microplastics at different depths utilizing a variety of frameworks and parameters[34–36,45,46,61,87,95,101] (Fig. 3a). Understanding how well these models reflect observed water-column microplastic patterns is key to elucidating dispersal mechanisms and identifying sources of error and uncertainty in subsurface microplastic estimates.

In most models, vertical microplastic transport is governed by wind-induced mixing and large-scale three-dimensional advection processes (Fig. 3a). However, submesoscale (1–10 km) dynamics, such as eddy-driven advection—which are critical for the downwards transport of small oceanic particles[19]—are rarely parameterized[35,36]. Including submesoscale dynamics in future models could improve our understanding of small microplastic vertical transport and its variability.

Similarly, biological processes, including biofouling, marine snow formation and faecal pellet production—which enhance the gravitational sinking of microplastics[20]—are rarely taken into account[34,45,46]. When included, these processes are often modelled using temperature-dependent remineralization rates and constant grazing rates. However, regional variations in ecosystem structure[102], which significantly influence rates, are generally omitted. In addition, biogenic minerals (for example, calcium carbonate, hydrated silica and celestite), known to be critical ballasting factors driving the absolute flux of sinking particles[43,102], are overlooked in all models. Models commonly assume that microplastics are spherical and buoyant particles (Fig. 3a), despite observations of both buoyant and dense plastics of varying shapes with large differences in surface area to volume ratios. Such parameterizations contribute to discrepancies between model outputs and observations. For example, although observations reveal subsurface maxima of microplastics from epipelagic to abyssal depths[3,4,25,68,72,103], some models suggest that most microplastics might only reach depths ranging from 150 m to 1,000 m on a global scale[36,95] or within specific marine regimes[46]. Similarly, models indicate limited or even an absence of transport of microplastics to polar regions[34,95].

The sparse and uncertain measurements (discussed below) of subsurface microplastics makes it difficult to accurately evaluate the model performance and other parameterizations. Despite these challenges, models consistently emphasize the role of microplastic size in influencing their vertical distribution, aligning with our analysis[35,45,46,61] (Fig. 1b,c). For example, in the eastern North Pacific Ocean, microplastic sizes decrease towards the gyre centre, a trend predicted by models and confirmed by observations[25,35]. Similarly, in the Mediterranean, models predict that small water-column microplastics tend to reach the open ocean, primarily owing to the fast removal of large microplastics from coastal environments[61].

These results underscore the need for diverse empirical data on microplastics. Such data should include, but not be limited to, reliable measurements of abundance and characteristics, environmentally relevant sinking rates, biofouling rates, incorporation-detachment rates from aggregates, and the structural integrity and degradation rates of plastic-laden aggregates. Data on zooplankton microplastic particle selection and ingestion, categorized by grazing strategy, would also be invaluable to improving estimates of faecal pellet transport.

Polymer composition of subsurface microplastics

Over 56 polymer types have been detected in our synthesized dataset (Supplementary Table 6). Buoyant polymers, constituting half of global plastic production[104], dominate the subsurface microplastics synthesized in this study (Fig. 3b). But subsurface microplastics denser than seawater are more abundant offshore than nearshore ($P = 8 \times 10^{-4}$; Fig. 3b), probably owing to their higher fragmentation susceptibility[25]. Dense polymers typically have higher glass transition temperatures (T_g) than buoyant plastics. T_g is a critical parameter below which plastic becomes rigid and brittle, and above which it turns rubbery or viscous. This property increases the likelihood of surface erosion in dense polymers, leading to their fragmentation into smaller particles[105]. Dense microplastics were found to be skewed towards smaller size fractions compared with buoyant ones in the North Pacific Subtropical Gyre[25]. Considering this, certain processes could further expedite the fragmentation of dense plastics. Land-based dense plastic containers (for example, PET bottles), which can take years to reach offshore gyres[92,106,107], undergo extended weathering and degradation, intensifying their fragmentation. A study in the North Pacific Subtropical Gyre found that almost half of the plastics with identified production dates dated back to the twentieth century, showing decades-long persistence[108] and potential for microplastic release. A significant rise in dense plastics such as nylon and polyester, often linked to fishing activity[4], is noted offshore ($P = 0.001$ and $P = 0.004$; Fig. 3c). The atmosphere–ocean influx of microplastics, estimated to range from 0.013 million metric tons to 25 million metric tons annually[109], may also contribute, with polyester comprising a significant fraction of airborne microplastics[110].

Another notable finding is the apparent decline in the portions of buoyant polypropylene submerged in the water column compared with the apparent increase in polyethylene offshore ($P = 2 \times 10^{-4}$ and $P = 1.9 \times 10^{-7}$; Fig. 3c), indicating faster polypropylene removal. Ultraviolet stability may contribute to polyethylene fragmenting less and remaining longer at sea, whereas the tertiary carbon in the polypropylene backbone makes it more vulnerable to abiotic degradation[111]. Photodegradation experiments have documented that polypropylene fragments and produces dissolved organic carbon faster than polyethylene in seawater[112,113]. These findings highlight the varying environmental degradation potential of different marine plastics.

Uncertainty sources and improvement strategies

Uncertainties in quantifying subsurface microplastics in the ocean water column stem from several factors. First, observational data on subsurface microplastics are modest and unevenly distributed owing to sampling challenges and time-consuming analysis. Compared with floating plastics[2], data on subsurface plastics remain limited (Fig. 1a). Variations in microplastic concentrations with depth underline the importance of obtaining higher-resolution depth-resolved samples. However, collecting microplastics at different depths requires specialized tools that are not always accessible to the research community (Extended Data Table 1). In addition, ship time is required for sufficient sampling with depth, creating a trade-off between maximizing depth versus horizontal sample resolution. Collectively, these factors contribute to observational data paucity, causing the uncertainties in estimating global patterns. Second, uncertainties arise from inconsistent analysis methodologies, as highlighted in

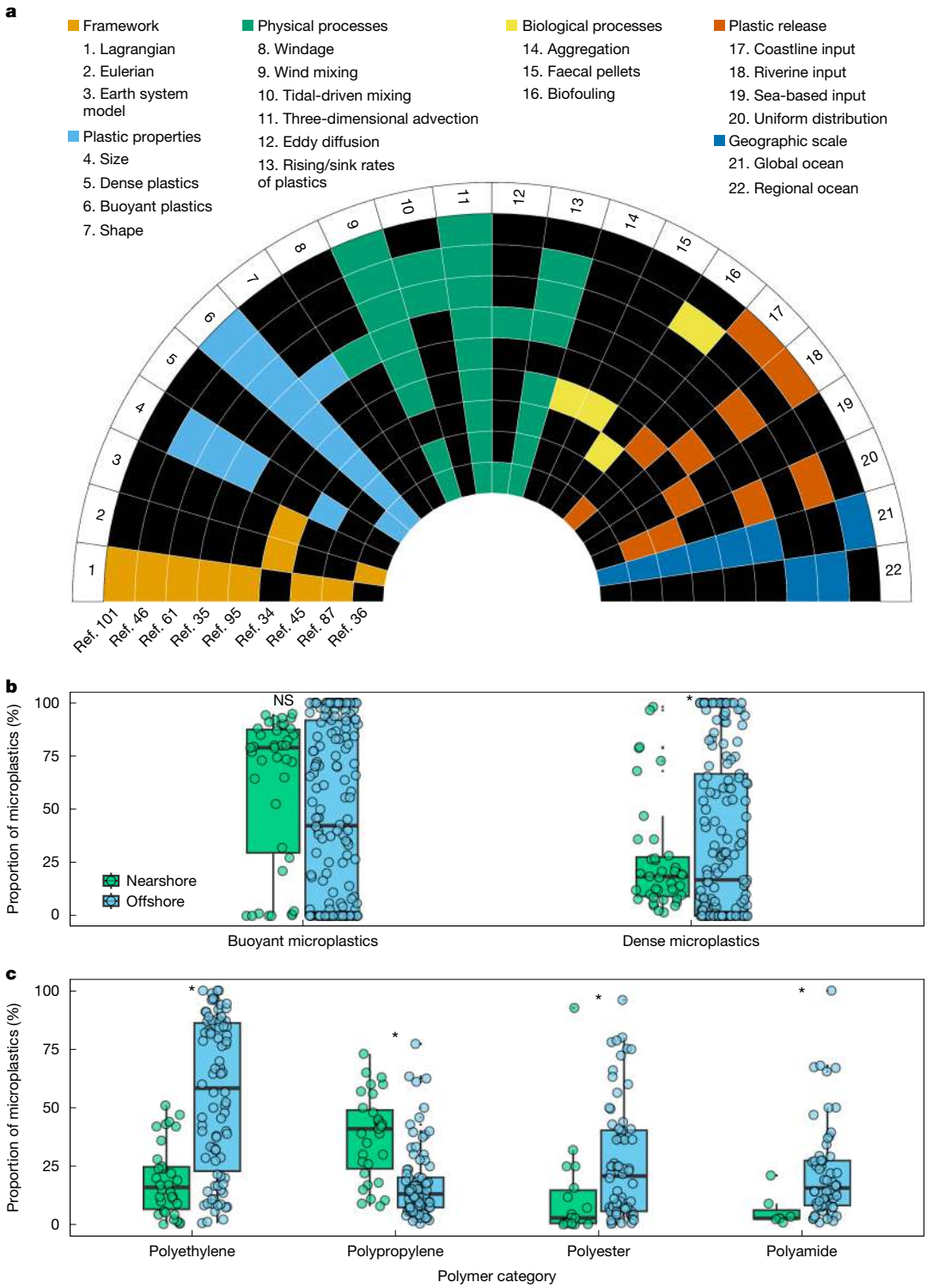

Fig. 3 | Comparison between the specifications of modelling studies and polymer compositions as functions of sampling locations. a, The available model parameters for simulating the transport, distribution and fate of microplastics in the three-dimensional ocean from refs. 34–36,45,46,61,87,95,101. Various model frameworks, including Lagrangian and Eulerian ocean models, and coupled Earth system models, have been used in research with different aims. These models incorporate different parameters influencing microplastic transport, such as plastic properties (for example, size, shape and density), oceanic physical processes (for example, mixing, advection and diffusion), biological factors (for example, biofouling, aggregation and faecal pellets), as well as scenarios of plastic inputs and spatial scales. **b**, Proportions of buoyant and dense microplastics in nearshore and offshore waters. Data were compiled from 18 peer-reviewed papers on water-column microplastics that provided polymer compositions[3,4,6,15,16,25,33,60,67,68,72,83,126,127,129–132]. Polymers with densities lower than natural seawater ($\rho = 1.025$ g cm^{-3}) are defined as buoyant polymers whereas dense polymers have a density greater than natural seawater. **c**, Proportions of polyethylene, polypropylene, polyester and polyamide microplastics in the water column in nearshore and offshore. Bold black horizontal lines within the coloured boxes represent the boxplot medians, while the top and bottom of the boxes indicate the 25th and 75th percentiles. The whiskers indicate the largest and smallest measured values within 1.5 interquartile ranges from the box. The asterisk indicates the statistically significant differences among different polymer categories ($P < 0.05$).

Extended Data Table 1, and Supplementary Tables 2 and 3. Differences in sample collection, purification, particle size limit, polymer identification approaches and corresponding extrapolation can lead to divergent results. Moreover, particle loss or contamination during sample preprocessing and transport further compromises result robustness. Finally, data processing and reporting influence the accuracy and comparability of microplastic determinations. Variations in spectral collection approaches and libraries significantly affect the accuracy of microplastic identification[26,114]. The main challenge in data reporting is the limited availability of original datasets detailing microplastic abundance, size and polymer type, hindering data standardization for meaningful comparison.

Enhancing sampling efforts and harmonizing methodologies are crucial steps to mitigate the existing uncertainties. Interdisciplinary collaboration and resource-sharing are essential, given the sampling challenges. Joint research cruises, multi-institutional collaborations and coordinated, targeted sampling campaigns can improve spatial coverage and depth resolution. Recent programmes on plastic pollution in coral-reef[115] and freshwater[116] ecosystems have yielded consistent datasets through global sample collection and standardized methods[23]. Collaboration between scientists focused on marine particles research to standardize sampling strategies across multiple regions can greatly benefit water-column microplastic studies. Established marine particulate research protocols[117], such as trace-metal clean protocols, offer efficient procedures for sample collection and preservation. Sharing both new and archived particulate samples can enhance sample resolution for microplastic analysis. In addition, developing camera/optical-sensor-based techniques on autonomous platforms would enable continuous, high-resolution monitoring. For harmonized microplastic analysis, we recommend employing chemical imaging (for example, μ-FTIR imaging)[3,118] followed by semi-automated data analysis with open-source reference spectrum libraries[119,120] to identify particles smaller than 100 μm in each sample without subsampling. This minimizes human bias and allows for effective identification and quantification of microplastics down to 10 μm. For large microplastics, μ-Raman/FTIR combined with visual microscopic inspection can be applied for single-particle analysis, requiring no specific sample preparation or advanced skills. Besides improving observational coverage, refining current models and incorporating new parameterizations are necessary to enhance confidence in global projections of microplastic distributions across depths.

Conclusion

Microplastics in the ocean are mostly irretrievable and persistent[1,9]. Our synthesis of subsurface microplastic observations over a 10-year period generates a global benchmark (Table 1). Despite observational uncertainties, the substantial presence of subsurface microplastics in both nearshore and offshore waters underscores the ocean water column as a critical yet uncharacterized reservoir of plastics. Small microplastics show a gradual decrease in abundance with depth, suggesting a more uniform distribution and longer lifespan in the water column, whereas large microplastics are more effectively trapped by stratification. Offshore surface accumulation zones[37] extend into subsurface waters but are primarily composed of large microplastics. Such size-dependent transport patterns align with existing models[35,45,46,61]. The prolonged presence and accumulation of microplastics pose risks to the marine biome, where substantial knowledge gaps persist[1], and may impact biogeochemical cycles and isotopic measurements. This analysis highlights the urgent need for consistent methodologies, finer-scale investigations and broader international coordination to establish comprehensive, long-term monitoring and more accurate model projections. These efforts will improve understanding of microplastic dispersion, fate and impacts, aiding in formulating effective policies and management strategies.

Online content

Any methods, additional references, Nature Portfolio reporting summaries, source data, extended data, supplementary information, acknowledgements, peer review information; details of author contributions and competing interests; and statements of data and code availability are available at https://doi.org/10.1038/s41586-025-08818-1.

1. Thompson, R. C. et al. Twenty years of microplastic pollution research—what have we learned? *Science* **386**, eadl2746 (2024).
2. Eriksen, M. et al. A growing plastic smog, now estimated to be over 170 trillion plastic particles afloat in the world's oceans—urgent solutions required. *PLoS ONE* **18**, e0281596 (2023).
3. Zhao, S. et al. Large quantities of small microplastics permeate the surface ocean to abyssal depths in the South Atlantic Gyre. *Glob. Change Biol.* **28**, 2991–3006 (2022).
4. Tekman, M. B. et al. Tying up loose ends of microplastic pollution in the Arctic: distribution from the sea surface through the water column to deep-sea sediments at the HAUSGARTEN observatory. *Environ. Sci. Technol.* **54**, 4079–4090 (2020).
5. Isobe, A. et al. A multilevel dataset of microplastic abundance in the world's upper ocean and the Laurentian Great Lakes. *Microplast. Nanoplast.* **1**, 16 (2021).
6. Egger, M., Sulu-Gambari, F. & Lebreton, L. First evidence of plastic fallout from the North Pacific Garbage Patch. *Sci. Rep.* **10**, 7495 (2020).
7. Villarrubia-Gómez, P., Cornell, S. E. & Fabres, J. Marine plastic pollution as a planetary boundary threat—the drifting piece in the sustainability puzzle. *Mar. Policy* **96**, 213–220 (2018).
8. Reddy, S. & Lau, W. *Breaking the Plastic Wave: A Comprehensive Assessment of Pathways Towards Stopping Ocean Plastic Pollution* (PEW Charitable Trusts, 2020).
9. Law, K. L. Plastics in the marine environment. *Ann. Rev. Mar. Sci.* **9**, 205–229 (2017).
10. MacLeod, M., Arp, H. P. H., Tekman, M. B. & Jahnke, A. The global threat from plastic pollution. *Science* **373**, 61–65 (2021).
11. Andrady, A. L. The plastic in microplastics: a review. *Mar. Pollut. Bull.* **119**, 12–22 (2017).
12. Rochman, C. M. et al. Rethinking microplastics as a diverse contaminant suite. *Environ. Toxicol. Chem.* **38**, 703–711 (2019).
13. Van Sebille, E. et al. The physical oceanography of the transport of floating marine debris. *Environ. Res. Lett.* **15**, 023003 (2020).
14. Kane, I. A. et al. Seafloor microplastic hotspots controlled by deep-sea circulation. *Science* **368**, 1140–1145 (2020).
15. Ross, P. S. et al. Pervasive distribution of polyester fibres in the Arctic Ocean is driven by Atlantic inputs. *Nat. Commun.* **12**, 106 (2021).
16. Pabortsava, K. & Lampitt, R. S. High concentrations of plastic hidden beneath the surface of the Atlantic Ocean. *Nat. Commun.* **11**, 4073 (2020).
17. Lal, D. The oceanic microcosm of particles: suspended particulate matter, about 1 gram in 100 tons of seawater, plays a vital role in ocean chemistry. *Science* **198**, 997–1009 (1977).
18. IPCC: Summary for Policymakers. In *Climate Change 2021: The Physical Science Basis* (eds Masson-Delmotte, V. et al.) (Cambridge Univ. Press, 2021).
19. Boyd, P. W., Claustre, H., Levy, M., Siegel, D. A. & Weber, T. Multi-faceted particle pumps drive carbon sequestration in the ocean. *Nature* **568**, 327–335 (2019).
20. Galloway, T. S., Cole, M. & Lewis, C. Interactions of microplastic debris throughout the marine ecosystem. *Nat. Ecol. Evol.* **1**, 0116 (2017).
21. Ziervogel, K. et al. Microbial interactions with microplastics: Insights into the plastic carbon cycle in the ocean. *Mar. Chem.* **262**, 104395 (2024).
22. Galgani, L. et al. Hitchhiking into the deep: how microplastic particles are exported through the biological carbon pump in the North Atlantic Ocean. *Environ. Sci. Technol.* **56**, 15638–15649 (2022).
23. Law, K. L. & Rochman, C. M. Large-scale collaborations uncover global extent of plastic pollution. *Nature* **169**, 254–255 (2023).
24. Koelmans, A. A. et al. Risk assessment of microplastic particles. *Nat. Rev. Mater.* **7**, 138–152 (2022).
25. Zhao, S., Mincer, T. J., Lebreton, L. & Egger, M. Pelagic microplastics in the North Pacific Subtropical Gyre: a prevalent anthropogenic component of the particulate organic carbon pool. *PNAS Nexus* **2**, pgad070 (2023).
26. Primpke, S. et al. Critical assessment of analytical methods for the harmonized and cost-efficient analysis of microplastics. *Appl. Spectrosc.* **74**, 1012–1047 (2020).
27. Peeken, I. et al. Arctic sea ice is an important temporal sink and means of transport for microplastic. *Nat. Commun.* **9**, 1505 (2018).
28. Obbard, R. W. et al. Global warming releases microplastic legacy frozen in Arctic Sea ice. *Earths Future* **2**, 315–320 (2014).
29. Roscher, L. et al. Microplastic pollution in the Weser Estuary and the German North Sea. *Environ. Pollut.* **288**, 117681 (2021).
30. Abel, S. M., Primpke, S., Int-Veen, I., Brandt, A. & Gerdts, G. Systematic identification of microplastics in abyssal and hadal sediments of the Kuril Kamchatka Trench. *Environ. Pollut.* **269**, 116095 (2021).
31. Courtene-Jones, W., van Gennip, S., Penicaud, J., Penn, E. & Thompson, R. C. Synthetic microplastic abundance and composition along a longitudinal gradient traversing the subtropical gyre in the North Atlantic Ocean. *Mar. Pollut. Bull.* **185**, 114371 (2022).
32. Molazadeh, M. et al. The role of turbulence in the deposition of intrinsically buoyant MPs. *Sci. Total Environ.* **911**, 168540 (2024).
33. Song, Y. K. et al. Horizontal and vertical distribution of microplastics in Korean coastal waters. *Environ. Sci. Technol.* **52**, 12188–12197 (2018).
34. Kvale, K., Prowe, A. F., Chien, C.-T., Landolfi, A. & Oschlies, A. The global biological microplastic particle sink. *Sci Rep.* **10**, 16670–1 (2020).
35. Klink, D., Peytavin, A. & Lebreton, L. Size dependent transport of floating plastics modeled in the global ocean. *Front. Mar. Sci.* **9**, 903134 (2022).

36. Mountford, A. & Morales Maqueda, M. Eulerian modeling of the three-dimensional distribution of seven popular microplastic types in the global ocean. *J. Geophys. Res. Oceans* **124**, 8558–8573 (2019).
37. Van Sebille, E. et al. A global inventory of small floating plastic debris. *Environ. Res. Lett.* **10**, 124006 (2015).
38. Amenábar, M. et al. Spatial distribution of microplastics in a coastal upwelling region: offshore dispersal from urban sources in the Humboldt Current System. *Environ. Pollut.* **343**, 123157 (2024).
39. Cael, B., Cavan, E. L. & Britten, G. L. Reconciling the size-dependence of marine particle sinking speed. *Geophys. Res. Lett.* **48**, e2020GL091771 (2021).
40. Armbrust, E. V. The life of diatoms in the world's oceans. *Nature* **459**, 185–192 (2009).
41. Amaral-Zettler, L. A., Zettler, E. R. & Mincer, T. J. Ecology of the plastisphere. *Nat. Rev. Microbiol.* **18**, 139–151 (2020).
42. Amaral-Zettler, L. A., Zettler, E. R., Mincer, T. J., Klaassen, M. A. & Gallager, S. M. Biofouling impacts on polyethylene density and sinking in coastal waters: a macro/micro tipping point? *Water Res.* **201**, 117289 (2021).
43. Sun, X.-F., Zhang, Y., Xie, M.-Y., Mai, L. & Zeng, E. Y. Calcite carbonate sinks low-density plastic debris in open oceans. *Nat. Commun.* **15**, 4837 (2024).
44. Egger, M. et al. A spatially variable scarcity of floating microplastics in the eastern North Pacific Ocean. *Environ. Res. Lett.* **15**, 114056 (2020).
45. Lobelle, D. et al. Global modeled sinking characteristics of biofouled microplastic. *J. Geophys. Res. Oceans* **126**, e2020JC017098 (2021).
46. Fischer, R. et al. Modelling submerged biofouled microplastics and their vertical trajectories. *Biogeosciences* **19**, 2211–2234 (2022).
47. Reineccius, J. & Waniek, J. J. First long-term evidence of microplastic pollution in the deep subtropical Northeast Atlantic. *Environ. Pollut.* **305**, 119302 (2022).
48. Reineccius, J. et al. Abundance and characteristics of microfibers detected in sediment trap material from the deep subtropical North Atlantic Ocean. *Sci. Total Environ.* **738**, 140354 (2020).
49. Alurralde, G. et al. Anthropogenic microfibres flux in an Antarctic coastal ecosystem: the tip of an iceberg? *Mar. Pollut. Bull.* **175**, 113388 (2022).
50. Rowlands, E. et al. Vertical flux of microplastic, a case study in the Southern Ocean, South Georgia. *Mar. Pollut. Bull.* **193**, 115117 (2023).
51. Mateos-Cárdenas, A., Wheeler, A. J. & Lim, A. Microplastics and cellulosic microparticles in North Atlantic deep waters and in the cold-water coral *Lophelia pertusa*. *Mar. Pollut. Bull.* **206**, 116741 (2024).
52. Zhang, X., Liu, Z., Li, D., Zhao, Y. & Zhang, Y. Turbidity currents regulate the transport and settling of microplastics in a deep-sea submarine canyon. *Geology* **52**, 646–650 (2024).
53. Ikenoue, T., Nakajima, R., Osafune, S., Siswanto, E. & Honda, M. C. Vertical flux of microplastics in the deep subtropical Pacific Ocean: moored sediment-trap observations within the Kuroshio Extension Recirculation Gyre. *Environ. Sci. Technol.* **58**, 16121–16130 (2024).
54. Lam, P. J., Doney, S. C. & Bishop, J. K. The dynamic ocean biological pump: Insights from a global compilation of particulate organic carbon, $CaCO_3$, and opal concentration profiles from the mesopelagic. *Glob. Biogeochem. Cycles* **25**, GB3009 (2011).
55. Enders, K., Lenz, R., Stedmon, C. A. & Nielsen, T. G. Abundance, size and polymer composition of marine microplastics ≥ 10 µm in the Atlantic Ocean and their modelled vertical distribution. *Mar. Pollut. Bull.* **100**, 70–81 (2015).
56. Gunaalan, K. et al. Does water column stratification influence the vertical distribution of microplastics? *Environ. Pollut.* **340**, 122865 (2024).
57. Kooi, M., Nes, E. H. V., Scheffer, M. & Koelmans, A. A. Ups and downs in the ocean: effects of biofouling on vertical transport of microplastics. *Environ. Sci. Technol.* **51**, 7963–7971 (2017).
58. Dittmar, S., Ruhl, A. S., Altmann, K. & Jekel, M. Settling velocities of small microplastic fragments and fibers. *Environ. Sci. Technol.* **58**, 6359–6369 (2024).
59. Kaiser, D., Estelmann, A., Kowalski, N., Glockzin, M. & Waniek, J. J. Sinking velocity of sub-millimeter microplastic. *Mar. Pollut. Bull.* **139**, 214–220 (2019).
60. Egger, M. et al. Pelagic distribution of plastic debris (> 500 µm) and marine organisms in the upper layer of the North Atlantic Ocean. *Sci. Rep.* **12**, 13465 (2022).
61. Onink, V., Kaandorp, M. L., van Sebille, E. & Laufkötter, C. Influence of particle size and fragmentation on large-scale microplastic transport in the Mediterranean Sea. *Environ. Sci. Technol.* **56**, 15528–15540 (2022).
62. Hidalgo-Ruz, V., Gutow, L., Thompson, R. C. & Thiel, M. Microplastics in the marine environment: a review of the methods used for identification and quantification. *Environ. Sci. Technol.* **46**, 3060–3075 (2012).
63. Wright, R. J., Erni-Cassola, G., Zadjelovic, V., Latva, M. & Christie-Oleza, J. A. Marine plastic debris: a new surface for microbial colonization. *Environ. Sci. Technol.* **54**, 11657–11672 (2020).
64. Zhao, S., Zettler, E. R., Amaral-Zettler, L. A. & Mincer, T. J. Microbial carrying capacity and carbon biomass of plastic marine debris. *ISME J.* **15**, 67–77 (2021).
65. Doostmohammadi, A., Stocker, R. & Ardekani, A. M. Low-Reynolds-number swimming at pycnoclines. *Proc. Natl Acad. Sci. USA* **109**, 3856–3861 (2012).
66. MacIntyre, S., Alldredge, A. L. & Gotschalk, C. C. Accumulation of marines now at density discontinuities in the water column. *Limnol. Oceanogr.* **40**, 449–468 (1995).
67. Uurasjärvi, E., Pääkkönen, M., Setälä, O., Koistinen, A. & Lehtiniemi, M. Microplastics accumulate to thin layers in the stratified Baltic Sea. *Environ. Pollut.* **268**, 115700 (2021).
68. Zobkov, M., Esiukova, E., Zyubin, A. & Samusev, I. Microplastic content variation in water column: the observations employing a novel sampling tool in stratified Baltic Sea. *Mar. Pollut. Bull.* **138**, 193–205 (2019).
69. Manullang, C. Y. et al. Vertical distribution of microplastic along the main gate of Indonesian Throughflow pathways. *Mar. Pollut. Bull.* **199**, 115954 (2024).
70. Zhou, Q. et al. Trapping of microplastics in halocline and turbidity layers of the semi-enclosed Baltic Sea. *Front. Mar. Sci.* **8**, 761566 (2021).
71. Carlotti, F. et al. Microplastics in the maximum chlorophyll layer along a north-south transect in the Mediterranean Sea in comparison with zooplankton concentrations. *Mar. Pollut. Bull.* **196**, 115614 (2023).
72. Choy, C. A. et al. The vertical distribution and biological transport of marine microplastics across the epipelagic and mesopelagic water column. *Sci. Rep.* **9**, 7843 (2019).
73. Ardekani, A. & Stocker, R. Stratlets: low Reynolds number point-force solutions in a stratified fluid. *Phys. Rev. Lett.* **105**, 084502 (2010).
74. Yick, K. Y., Torres, C. R., Peacock, T. & Stocker, R. Enhanced drag of a sphere settling in a stratified fluid at small Reynolds numbers. *J. Fluid Mech.* **632**, 49–68 (2009).
75. Mrokowska, M. M. Influence of pycnocline on settling behaviour of non-spherical particle and wake evolution. *Sci. Rep.* **10**, 20595 (2020).
76. Zhang, M., Xu, D., Liu, L., Wei, Y. & Gao, B. Vertical differentiation of microplastics influenced by thermal stratification in a deep reservoir. *Environ. Sci. Technol.* **57**, 6999–7008 (2023).
77. Li, C., Zhu, L., Wang, X., Liu, K. & Li, D. Cross-oceanic distribution and origin of microplastics in the subsurface water of the South China Sea and Eastern Indian Ocean. *Sci. Total Environ.* **805**, 150243 (2022).
78. Zhdanov, I. et al. Differences in the fate of surface and subsurface microplastics: a case study in the Central Atlantic. *J. Mar. Sci. Eng.* **11**, 210 (2023).
79. Zhang, S. et al. Distribution characteristics of microplastics in surface and subsurface Antarctic seawater. *Sci. Total Environ.* **838**, 156051 (2022).
80. Morgana, S. et al. Microplastics in the Arctic: a case study with sub-surface water and fish samples off Northeast Greenland. *Environ. Pollut.* **242**, 1078–1086 (2018).
81. Pakhomova, S. et al. Microplastic variability in subsurface water from the Arctic to Antarctica. *Environ. Pollut.* **298**, 118808 (2022).
82. Lusher, A. L., Tirelli, V., O'Connor, I. & Officer, R. Microplastics in Arctic polar waters: the first reported values of particles in surface and sub-surface samples. *Sci. Rep.* **5**, 14947 (2015).
83. Kanhai, L. D. K. et al. Microplastics in sub-surface waters of the Arctic Central Basin. *Mar. Pollut. Bull.* **130**, 8–18 (2018).
84. Kanhai, L. D. K., Officer, R., Lyashevska, O., Thompson, R. C. & O'Connor, I. Microplastic abundance, distribution and composition along a latitudinal gradient in the Atlantic Ocean. *Mar. Pollut. Bull.* **115**, 307–314 (2017).
85. Lusher, A. L., Burke, A., O'Connor, I. & Officer, R. Microplastic pollution in the Northeast Atlantic Ocean: validated and opportunistic sampling. *Mar. Pollut. Bull.* **88**, 325–333 (2014).
86. Yakushev, E. et al. Microplastics distribution in the Eurasian Arctic is affected by Atlantic waters and Siberian rivers. *Commun. Earth Environ.* **2**, 23 (2021).
87. Wichmann, D., Delandmeter, P. & van Sebille, E. Influence of near-surface currents on the global dispersal of marine microplastic. *J.Geophys. Res. Oceans* **124**, 6086–6096 (2019).
88. Bergmann, M. et al. Plastic pollution in the Arctic. *Nat. Rev. Earth Environ.* **3**, 323–337 (2022).
89. Eriksen, M. et al. Plastic pollution in the world's oceans: more than 5 trillion plastic pieces weighing over 250,000 tons afloat at sea. *PLoS ONE* **9**, e111913 (2014).
90. Cózar, A. et al. Plastic debris in the open ocean. *Proc. Natl Acad. Sci. USA* **111**, 10239–10244 (2014).
91. Law, K. L. et al. Plastic accumulation in the North Atlantic subtropical gyre. *Science* **329**, 1185–1188 (2010).
92. Lebreton, L.-M., Greer, S. & Borrero, J. C. Numerical modelling of floating debris in the world's oceans. *Mar. Pollut. Bull.* **64**, 653–661 (2012).
93. Maximenko, N., Hafner, J. & Niiler, P. Pathways of marine debris derived from trajectories of Lagrangian drifters. *Mar. Pollut. Bull.* **65**, 51–62 (2012).
94. Van Sebille, E., England, M. H. & Froyland, G. Origin, dynamics and evolution of ocean garbage patches from observed surface drifters. *Environ. Res. Lett.* **7**, 044040 (2012).
95. Huck, T. et al. Three-dimensional dispersion of neutral "plastic" particles in a global ocean model. *Front. Anal. Sci.* **2**, 868515 (2022).
96. Karl, D. M., Knauer, G. A. & Martin, J. H. Downward flux of particulate organic matter in the ocean: a particle decomposition paradox. *Nature* **332**, 438–441 (1988).
97. Vaksmaa, A. et al. Polyethylene degradation and assimilation by the marine yeast *Rhodotorula mucilaginosa*. *ISME Commun.* **3**, 68 (2023).
98. Seeley, M. E., Song, B., Passie, R. & Hale, R. C. Microplastics affect sedimentary microbial communities and nitrogen cycling. *Nat. Commun.* **11**, 2372 (2020).
99. Libby, W. F. Radiocarbon dating: the method is of increasing use to the archeologist, the geologist, the meteorologist, and the oceanographer. *Science* **133**, 621–629 (1961).
100. Heaton, T. J. et al. Radiocarbon: a key tracer for studying Earth's dynamo, climate system, carbon cycle, and Sun. *Science* **374**, eabd7096 (2021).
101. Bajon, R. et al. Influence of waves on the three-dimensional distribution of plastic in the ocean. *Mar. Pollut. Bull.* **187**, 114533 (2023).
102. Lima, I. D., Lam, P. J. & Doney, S. C. Dynamics of particulate organic carbon flux in a global ocean model. *Biogeosciences* **11**, 1177–1198 (2014).
103. Bagaev, A., Khatmullina, L. & Chubarenko, I. Anthropogenic microlitter in the Baltic Sea water column. *Mar. Pollut. Bull.* **129**, 918–923 (2018).
104. Geyer, R., Jambeck, J. R. & Law, K. L. Production, use, and fate of all plastics ever made. *Sci. Adv.* **3**, e1700782 (2017).
105. Min, K., Cuiffi, J. D. & Mathers, R. T. Ranking environmental degradation trends of plastic marine debris based on physical properties and molecular structure. *Nat. Commun.* **11**, 727 (2020).
106. Maximenko, N., Hafner, J., Kamachi, M. & MacFadyen, A. Numerical simulations of debris drift from the Great Japan Tsunami of 2011 and their verification with observational reports. *Mar. Pollut. Bull.* **132**, 5–25 (2018).
107. Gennip, S. J. V. et al. In search for the sources of plastic marine litter that contaminates the Easter Island ecoregion. *Sci. Rep.* **9**, 19662 (2019).
108. Lebreton, L. et al. Industrialised fishing nations largely contribute to floating plastic pollution in the North Pacific subtropical gyre. *Sci. Rep.* **12**, 12666 (2022).
109. Allen, D. et al. Microplastics and nanoplastics in the marine-atmosphere environment. *Nat. Rev. Earth Environ.* **3**, 393–405 (2022).
110. Ortega, D. E. & Cortés-Arriagada, D. Atmospheric microplastics and nanoplastics as vectors of primary air pollutants—a theoretical study on the polyethylene terephthalate (PET) case. *Environ. Pollut.* **318**, 120860 (2023).

111. Gewert, B., Plassmann, M. M. & MacLeod, M. Pathways for degradation of plastic polymers floating in the marine environment. *Environ. Sci. Process. Impacts* **17**, 1513–1521 (2015).
112. Zhu, L., Zhao, S., Bittar, T. B., Stubbins, A. & Li, D. Photochemical dissolution of buoyant microplastics to dissolved organic carbon: rates and microbial impacts. *J. Hazard. Mater.* **383**, 121065 (2020).
113. Delre, A. et al. Plastic photodegradation under simulated marine conditions. *Mar. Pollut. Bull.* **187**, 114544 (2023).
114. De Frond, H. et al. What determines accuracy of chemical identification when using microspectroscopy for the analysis of microplastics? *Chemosphere* **313**, 137300 (2023).
115. Pinheiro, H. T. et al. Plastic pollution on the world's coral reefs. *Nature* **619**, 311–316 (2023).
116. Nava, V. et al. Plastic debris in lakes and reservoirs. *Nature* **619**, 317–322 (2023).
117. Hurd, D. C. & Spencer, D. W. (eds) *Marine Particles: Analysis and Characterization* Geophysical Monograph Series Vol. 63 (AGU, 1991).
118. Primpke, S., Lorenz, C., Rascher-Friesenhausen, R. & Gerdts, G. An automated approach for microplastics analysis using focal plane array (FPA) FTIR microscopy and image analysis. *Anal. Methods* **9**, 1499–1511 (2017).
119. Cowger, W. et al. Microplastic spectral classification needs an open source community: open specy to the rescue! *Anal. Chem.* **93**, 7543–7548 (2021).
120. Primpke, S. et al. Toward the systematic identification of microplastics in the environment: evaluation of a new independent software tool (siMPle) for spectroscopic analysis. *Appl. Spectrosc.* **74**, 1127–1138 (2020).
121. Materić, D., Holzinger, R. & Niemann, H. Nanoplastics and ultrafine microplastic in the Dutch Wadden Sea—the hidden plastics debris? *Sci. Total Environ.* **846**, 157371 (2022).
122. Kukulka, T., Proskurowski, G., Morét-Ferguson, S., Meyer, D. W. & Law, K. L. The effect of wind mixing on the vertical distribution of buoyant plastic debris. *Geophys. Res. Lett.* **39**, L07601 (2012).
123. Cole, M. et al. Microplastics alter the properties and sinking rates of zooplankton faecal pellets. *Environ. Sci. Technol.* **50**, 3239–3246 (2016).
124. Bohdan, K. Estimating global marine surface microplastic abundance: systematic literature review. *Sci. Total Environ.* **832**, 155064 (2022).
125. Lebreton, L. The status and fate of oceanic garbage patches. *Nat. Rev. Earth Environ.* **3**, 730–732 (2022).
126. Wang, X., Zhu, L., Liu, K. & Li, D. Prevalence of microplastic fibers in the marginal sea water column off southeast China. *Sci. Total Environ.* **804**, 150138 (2022).
127. Ding, J. et al. Microplastics in the coral reef systems from Xisha Islands of South China Sea. *Environ. Sci. Technol.* **53**, 8036–8046 (2019).
128. Dai, Z. et al. Occurrence of microplastics in the water column and sediment in an inland sea affected by intensive anthropogenic activities. *Environ. Pollut.* **242**, 1557–1565 (2018).
129. Cordova, M. & Hernawan, U. Microplastics in Sumba waters, East Nusa Tenggara. In *IOP Conference Series: Earth and Environmental Science* Vol. 162, 012023 (IOP, 2018).
130. Oztekin, A. & Bat, L. Microlitter pollution in sea water: a preliminary study from Sinop Sarikum coast of the southern Black Sea. *Turkish J. Fish. Aquat. Sci.* **17**, 1431–1440 (2017).
131. Li, D. et al. Profiling the vertical transport of microplastics in the West Pacific Ocean and the East Indian Ocean with a novel in situ filtration technique. *Environ. Sci. Technol.* **54**, 12979–12988 (2020).
132. Reisser, J. et al. The vertical distribution of buoyant plastics at sea: an observational study in the North Atlantic Gyre. *Biogeosciences* **12**, 1249–1256 (2015).
133. Wiesinger, H., Wang, Z. & Hellweg, S. Deep dive into plastic monomers, additives, and processing aids. *Environ. Sci. Technol.* **55**, 9339–9351 (2021).

Analysis

Methods

Categorization

Small and large microplastics. Our analysis categorizes microplastics into two size class, small (<100 µm) and large (>100 µm), based on previous laboratory[59,73] and field[3,4,16,25] analyses, as well as modelling results[35,45,46,61]. Experimental evidence and mathematical models indicate that the relationship between settling velocity and particle size is described by quadratic linear regression, despite the influence of particle shape and density[58,59,73]. Once marine sinking particles and microplastics decrease below 100 µm, the settling velocities of different plastic polymers converge, typically differing by less than one order of magnitude (see Fig. 1 in ref. 39, Fig. 2 in ref. 59 and Fig. 3 in ref. 58). In addition, particles under 100 µm are less affected by the omnipresent density stratification, which generally hinders particle vertical motion[73]. Numerous modelling studies on the vertical transport of microplastics have demonstrated distinct behaviours for particles smaller than 100 µm compared with large particles[35,45,46,61]. Finally, field observations, using advanced identification techniques such as chemical imaging, further confirm that microplastics smaller than 100 µm dominate marine plastic debris globally, accounting for up to 80% of total plastic particles[3,4,25,55].

Using '100 m' as the reference depth for large-microplastics accumulation zone at depth. We identify subsurface microplastic accumulation in the 1–60-m depth range, where measurements from one reference were collected at a single depth (shown as light blue dots in Fig. 1a,b). Elevated subsurface microplastic abundances at 1–60-m depth at mid-latitudes corresponds to well-documented surface convergence zones at the sea surface within subtropical gyres[92–94]. This surface accumulation zone is reflected in our study, where floating microplastics of a comparable size fraction were collected at 0–50-cm depth with surface net tows (Fig. 1a,b). Data from the 0.5–1-m range are absent owing to discontinuities in sample collections along the water depth in the literature. This indicates that plastic accumulation zones stretch from the surface into the ocean water column. The existence of patches of large microplastics in the near-surface waters is mainly attributed to a combination of wind-driven Ekman currents and prolonged residence in the upper water layers enabled by the strong buoyancy of large-sized plastics[35,95].

To investigate whether datasets from studies collecting subsurface microplastics from multiple depths per station (dark blue dots in Fig. 1a) could support our finding, we compare the abundances of microplastics across two categories: (1) large versus small microplastics; and (2) abundances above or below the water depth of 100 m. We chose 100 m as the lower boundary for the following reasons: (1) the upper 100-m layer is where the majority of wind-driven mixing occurs[36,87]; and (2) the lower boundary of the sunlit euphotic zone is at 100 m, a depth typically used as a reference for assessing the POC flux via the ocean's biological carbon pump. Below 100 m, the consumption of organic-matter-associated particles varies significantly between oceanic provinces[134]. As biological processes are one of the main mechanisms for the vertical transport of microplastics, using 100 m as the boundary allows us to constrain variations in the biological factors when comparing microplastic abundances.

Search term. We acknowledge the possibility of inadvertent omissions. To ensure thoroughness in retrieving scientific articles containing quantitative subsurface microplastics data into the oceanic water column, the following search pattern was constructed for Web of Science (www.webofscience.com):

TS = (microplastic$ or microlitter or "micro plastic$" or "plastic particle$" or "plastic fragments" or "resin pellet$" or "plastic particle$") and TS = (subsurface$ or subsurface$ or vertical$ or water column$) and ab = (marine or ocean$ or sea or seawater or coast$).

Inclusion and exclusion criteria for literature studies on subsurface microplastics. The estimates of microplastics in the water column show considerable variability, primarily stemming from inconsistent methodologies and human errors. To construct a robust dataset, this study focuses exclusively on research targeting subsurface microplastics with clearly defined sampling depths.

Spectroscopy identification methods, such as Raman or FTIR, are widely used and offer a robust approach for microplastic analysis. Visual differentiation of particles smaller than 300 µm using optical microscopy alone is considered unreliable[26]. Studies relying solely on this method without spectroscopy (for example, Raman or FTIR) for plastics smaller than 100 µm were excluded. Studies with incomplete methodological descriptions—such as missing details on identification techniques, filter pore size or mesh specifications—were followed up with email enquiries. Articles were excluded if essential details were not provided in the response.

Detailed methodologies are available in Extended Data Table 1, and Supplementary Tables 2 and 3.

Data collection

For each study meeting the inclusion criteria, details such as mesh size, microplastic concentration, particle size distribution, sampling coordinates and sampling time were extracted into a spreadsheet. When this information was not directly available, data were obtained from maps and graphics within the articles using the 'WebPlotDigitizer' tool (https://github.com/ankitrohatgi/WebPlotDigitizer) to address data gaps. If no maps or graphics provided the required information, an email was sent to the corresponding author. Articles were excluded if no response was received with the necessary data. The complete dataset is publicly available in the 'Source data'.

Curating data to compare microplastics at depths of 1–60 m with those floating at the sea surface

For robust comparisons between microplastics in subsurface waters (1–60 m) and those at the sea surface within the upper 0.3-m layer (dataset from ref. 5), our analysis exclusively focuses on large microplastics. Floating microplastics at the sea surface are primarily sampled using surface net trawls with mesh sizes ranging from 200 µm to 300 µm (ref. 5). Therefore, microplastic concentrations in size fractions above 200 µm collected in near-surface waters were extracted from reviewed articles based on plastic size distribution data to facilitate the global comparisons. This refined dataset of microplastics in near-surface waters (n = 1257) comprises three size fractions: 5.3% (n = 67) of particles >200 µm, 78.7% (n = 989) of particles >250 µm, and 16.0% (n = 201) of particles >300 µm. The detailed information on the size fraction of microplastics in near-surface waters (1–60 m) is summarized in Supplementary Table 2. This approach also minimizes inconsistencies in the synthesized data collected from different projects, as some include fibrous microplastics in their estimates whereas others do not.

Building microplastic abundance distribution models

We fitted two GAMs to analyse the adjusted microplastic abundances in near-surface waters (1–60 m) and the floating microplastic abundances along the latitude gradient. To quantify prediction uncertainty, we employed a Monte Carlo simulation with 1,000 iterations. In each iteration, we resampled the data with replacement, fitted a GAM and predicted density values for 1,000 equally spaced latitude points. This process was repeated 1,000 times, generating a distribution of predictions. For each latitude, we calculated the mean and standard deviation of the predicted values to estimate central tendencies and uncertainties. This approach ensures robust predictions with uncertainty estimates across various resampling scenarios.

Power-law function for subsurface microplastic abundance profiles

A simple vertical model was built to replicate the observed plastic debris profiles in the water column of each study. This model is based on the measured relationship between microplastic abundances and water depth (Fig. 1c,d). In this approach, microplastic abundance is calculated as a function of water depth using the following equation: $\text{Abundance}_{\text{MP}} = 10^{a^{-1}\times[\log_{10}(\text{Waterdepth})-b]}$, where a and b represent the slope and intercept of the regression line obtained from the log–log plot of observed microplastics abundances against water depth.

Comparison of microplastic-C to total POC

The ratios of microplastic-C to total POC were measured in both the North Atlantic and North Pacific Subtropical gyres[25]. In the North Pacific, microplastic-C was estimated from in situ pump samples. The estimation process involved calculating particle mass based on polymer density and size (identified via μ-FTIR). This mass was then multiplied by the carbon content percentage (C%) of each polymer's chemical formula. Total POC data came from three stations in the North Pacific. At two of these stations, samples were filtered using 0.5-μm glass fibre filters at 6 depths (40–5,300 m) in August 2017 using in situ pumps, with POC calculated as the difference between total carbon and particulate inorganic carbon[135]. In addition, the total POC at ALOHA station was calculated by multiplying the total particulate carbon (TC) by the empirical POC:TC ratio (about 90%), which was measured at Station ALOHA[136]. The total particulate carbon data at Station ALOHA were from bottle samples at 10 different depths (from 5 m to 350 m) collected on 16 November 2018 during the cruise KM 18–21 (http://hahana.soest.hawaii.edu/hot/hot_jgofs.html). In the North Atlantic, microplastic-C was calculated using data from drifting sediment traps. Plastic mass in the traps was determined via pyrolysis gas chromatography–mass spectrometry, with carbon content based on each polymer's chemical formula. POC was measured from aliquots filtered onto combusted GF/F filters, which were exposed to fuming hydrochloric acid to remove carbonates. The dried filters were then analysed with an elemental analyser using an acetanilide standard. For more details on the method, the reader is referred to studies[22,25]. Finally, a log–log regression model is constructed to predict the relationship between microplastic-C and total POC as a function of water depth.

Statistical analysis

As the datasets were not normally distributed (Kolmogorov–Smirnov test) and lacked homogeneity of variances (Levene's test), the Kruskal–Wallis test, a non-parametric method, was used for multiple comparisons. When significant, pairwise comparisons were conducted with the Mann–Whitney–Wilcoxon test. Statistical significance was determined at $P < 0.05$. In addition, the mgcv, MASS and boot packages were used to fit the GAM, run the Monte Carlo simulations and do the bootstrap analysis. All statistical analyses and visualizations were performed using R software (v.3.4.3, R Development Core Team).

Data availability

All data supporting the findings of this study are available at https://doi.org/10.6084/m9.figshare.28157324 (ref. 137).

134. Buesseler, K. O., Boyd, P. W., Black, E. E. & Siegel, D. A. Metrics that matter for assessing the ocean biological carbon pump. *Proc. Natl Acad. Sci. USA* **117**, 9679–9687 (2020).
135. Subhas, A. V., Adkins, J. F., Dong, S., Rollins, N. E. & Berelson, W. M. The carbonic anhydrase activity of sinking and suspended particles in the North Pacific Ocean. *Limnol. Oceanogr.* **65**, 637–651 (2020).
136. Umhau, B. P. et al. Seasonal and spatial changes in carbon and nitrogen fluxes estimated using ^{234}Th: ^{238}U disequilibria in the North Pacific tropical and subtropical gyre. *Mar. Chem.* **217**, 103705 (2019).
137. Zhao, S. Datasets for submerged microplastics in the ocean. *figshare* https://doi.org/10.6084/m9.figshare.28157324 (2025).

Acknowledgements We thank E. van Sebille for advice. The following funding sources are acknowledged: L.A.A.-Z. and E.R.Z. acknowledge the financial support from the Netherlands Organisation for Scientific Research (NWO) in the frame of an NWO Groot project (OCENW.GROOT.2019.043); H.N. acknowledges European Research Council funding (ERC-CoG grant number 772923, project VORTEX); L.Z. and A.S. acknowledge the United States of America National Science Foundation (NSF EAGER OCE 2127669, NSF CBET 1910621); L.Z. acknowledges the China National Science Foundation (NSFC 42206154); M.T. acknowledges the European Union's Horizon 2020 research and innovation programme, MINKE project (under grant agreement number 101008724), and Global Challenges Research Fund (NE/V005448/1), project 'Reducing the Impacts of Plastic Waste in the Eastern Pacific Ocean' led by the University of Exeter, UK; R.P.B. acknowledges the Gordon and Betty Moore Foundation (#9208) and 2018 Star-Friedman grant for promising scientific research.

Author contributions S.Z.: conceptualization (lead), data curation (lead); formal analysis (lead); validation (lead); writing—original draft (lead); writing—review and editing (lead). K.F.K: validation (equal); writing—review and editing (equal). L.Z.: data curation (equal); formal analysis (equal); writing—review and editing (supporting). E.R.Z.: conceptualization (equal); validation (equal); writing—review and editing (equal). M.E.: conceptualization (equal); validation (supporting); writing—review and editing (supporting). T.J.M.: conceptualization (equal); validation (equal); writing—review and editing (supporting). L.A.A.-Z.: conceptualization (equal); validation (equal); writing—review and editing (equal). L.L.: validation (equal); writing—review and editing (equal). H.N.: validation (supporting); writing—review and editing (supporting). R.N.: validation (supporting); writing—review and editing (supporting). M.T.: validation (supporting); writing—review and editing (equal). R.P.B.: validation (supporting); writing—review and editing (supporting). L.G.: validation (supporting); writing—review and editing (supporting). A.S.: validation (supporting); writing—review and editing (equal).

Competing interests M.E. and L.L. are employed by The Ocean Cleanup, a non-profit organization aimed at advancing scientific understanding and developing solutions to rid the oceans of plastic.

Additional information

Supplementary information The online version contains supplementary material available at https://doi.org/10.1038/s41586-025-08818-1.

Correspondence and requests for materials should be addressed to Shiye Zhao.

Peer review information *Nature* thanks the anonymous reviewers for their contribution to the peer review of this work.

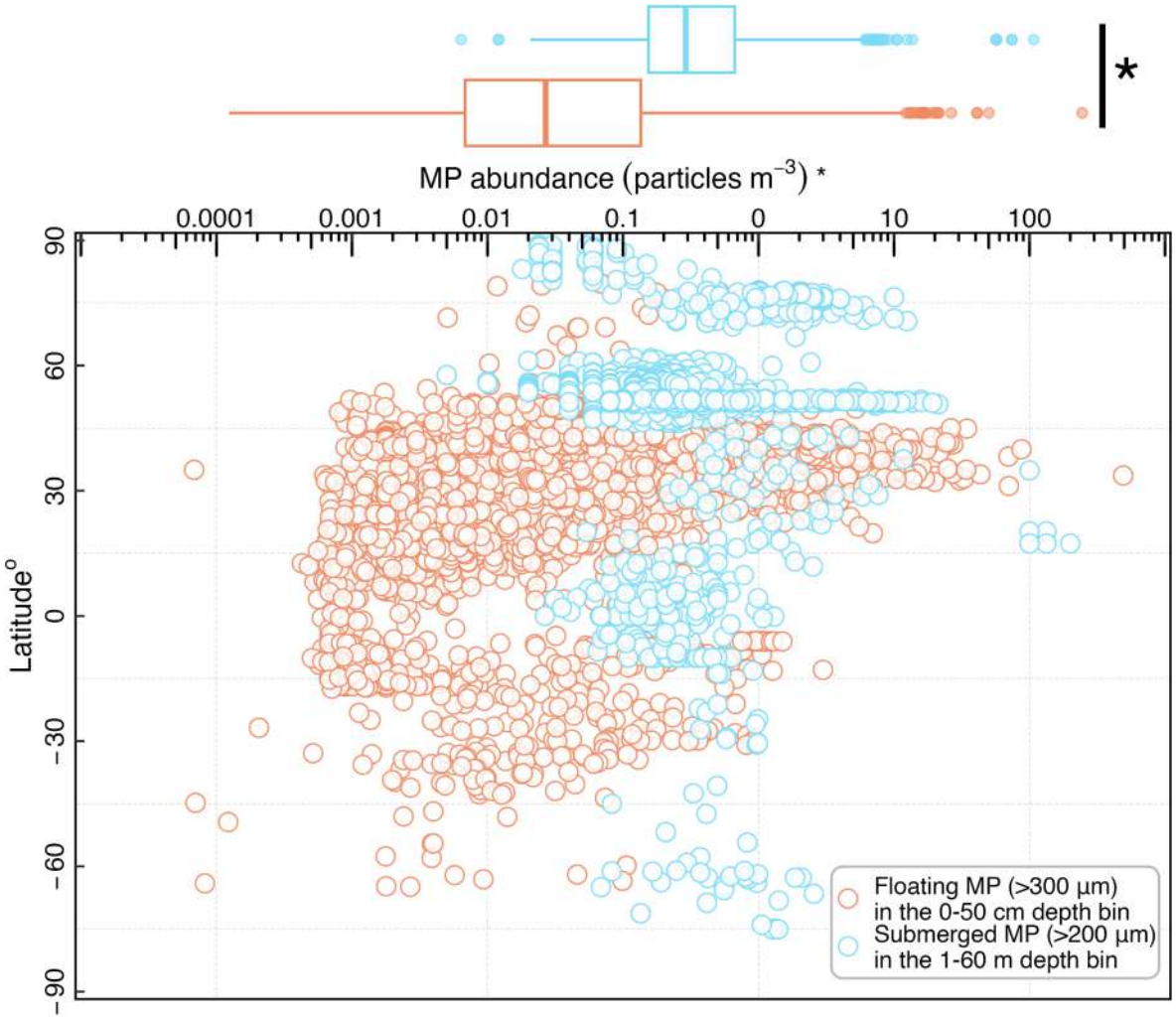

Extended Data Fig. 1 | Adjusted estimates of microplastic fragments (>200 µm) floating on the sea surface (orange dots) and in near-surface (blue dots) waters along latitudes. In the marginal boxplots, bold black horizontal lines represent medians of microplastics abundances; top and bottom of colored boxes represent 25th and 75th percentiles; and whiskers indicate the largest and the smallest measured values within 1.5 interquartile ranges from the box. Asterisks denote statistically significant differences between two categories (Mann-Whitney-Wilcoxon test, $p < .05$). This refined dataset of microplastics in the 1–60 m depth bin (n = 1257) comprises three size fractions: 5.3% (n = 67) of particles >200 µm, 78.7% (n = 989) of particles >250 µm, 16.0% (n = 201) of particles >300 µm. For more details, please refer to Methods, Fig. 1 and SI Table 2.

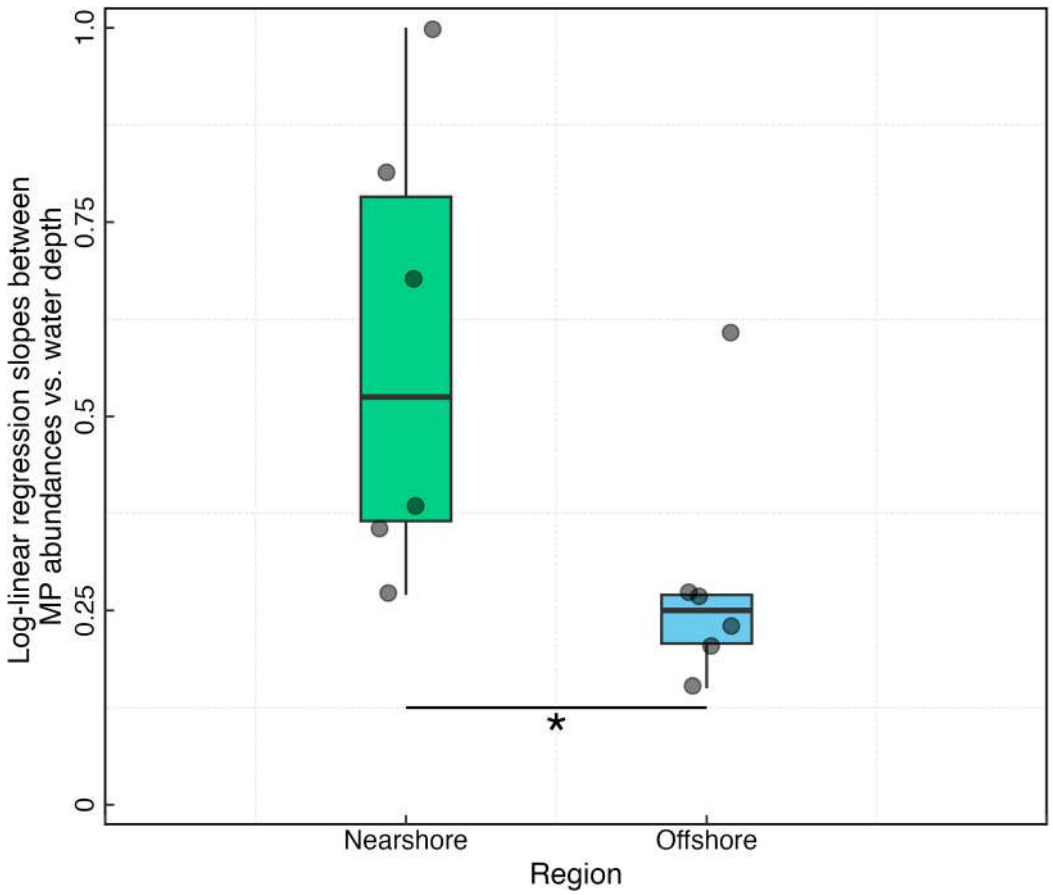

Extended Data Fig. 2 | Log-linear regression slopes between microplastics concentrations and water depth in nearshore (the brown boxplot) and offshore waters (the blue boxplot). Top and bottom of colored boxes represent 25th and 75th percentiles; and whiskers indicate the largest and the smallest measured values within 1.5 interquartile ranges from the box. Asterisks denote statistically significant differences between two groups (Mann-Whitney-Wilcoxon test, W = 32, P = 0.029).

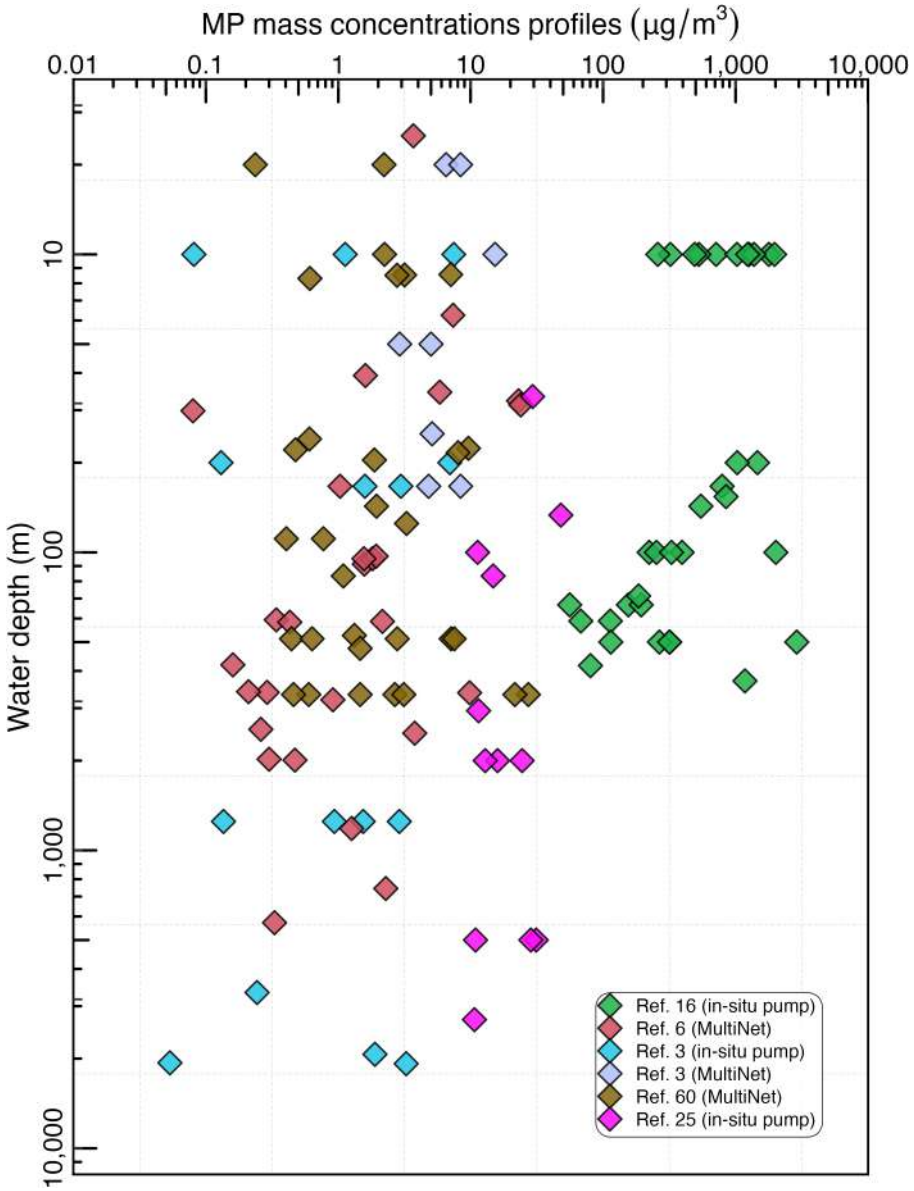

Extended Data Fig. 3 | Comparison of the mass concentrations of water column microplastics collected with the in-situ pump and MultiNet at the Atlantic Ocean and the eastern North Pacific Ocean. For each filter sample from the in-situ pump, μFTIR imaging were employed to analyze 1.8% (ref. 10, 16% (ref. 3) and 100% (ref. 25) of particles. In addition, the in-situ pump and MultiNet were deployed concurrently for collecting microplastics in the South Atlantic Subtropical Gyre[3] and the eastern North Pacific Subtropical Gyre[6,25].

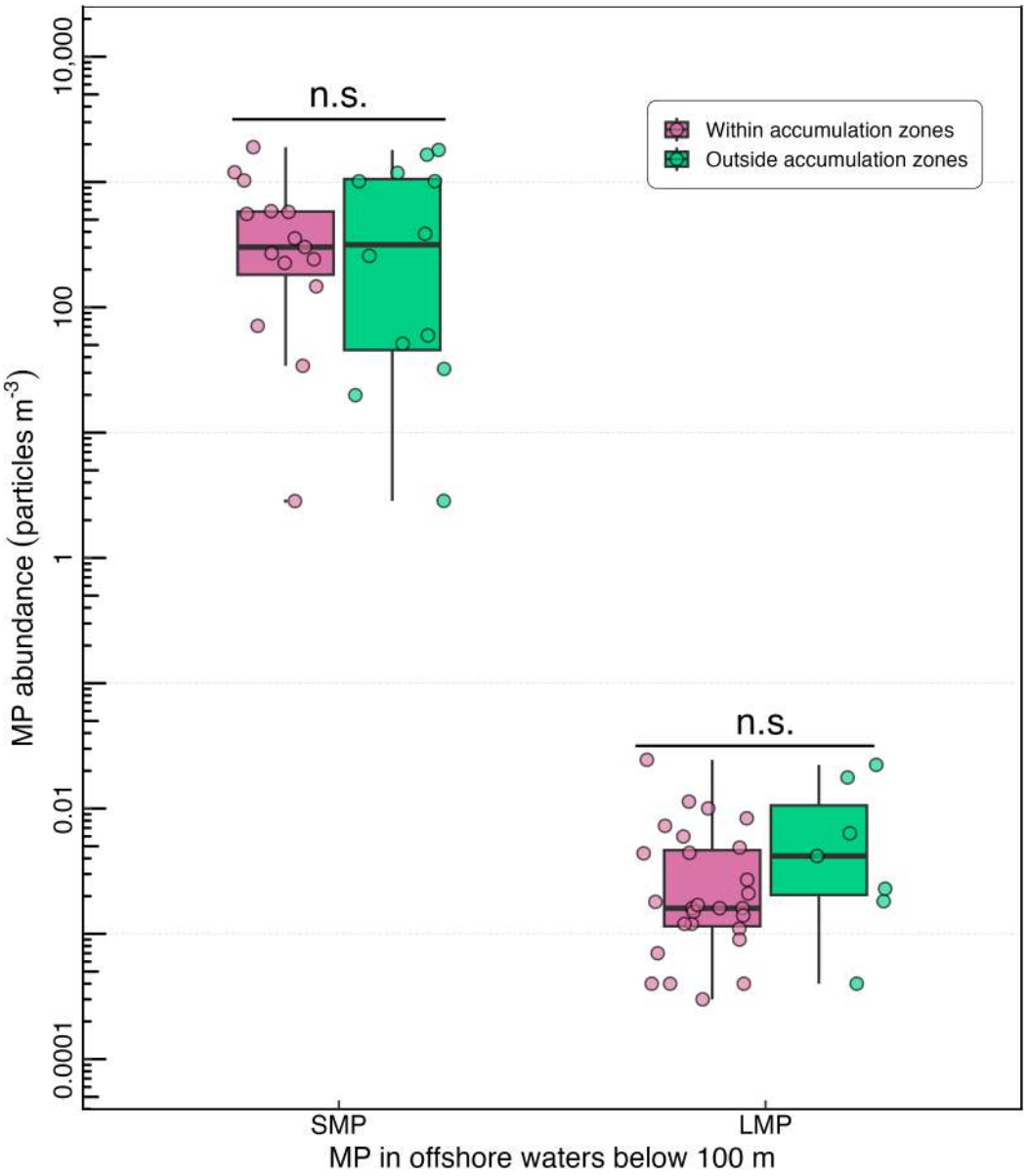

Extended Data Fig. 4 | The measured abundances of large and small microplastics within and outside the predicted offshore accumulation zones in the water column below 100 m. The boxplot medians are depicted by bold black horizontal lines, while the top and bottom of the colored boxes represent the 25th and 75th percentiles, respectively. The whiskers indicate the largest and smallest measured values within 1.5 interquartile ranges from the box. The datasets are from refs. 3,6,16,25,60. No statistical differences are found.

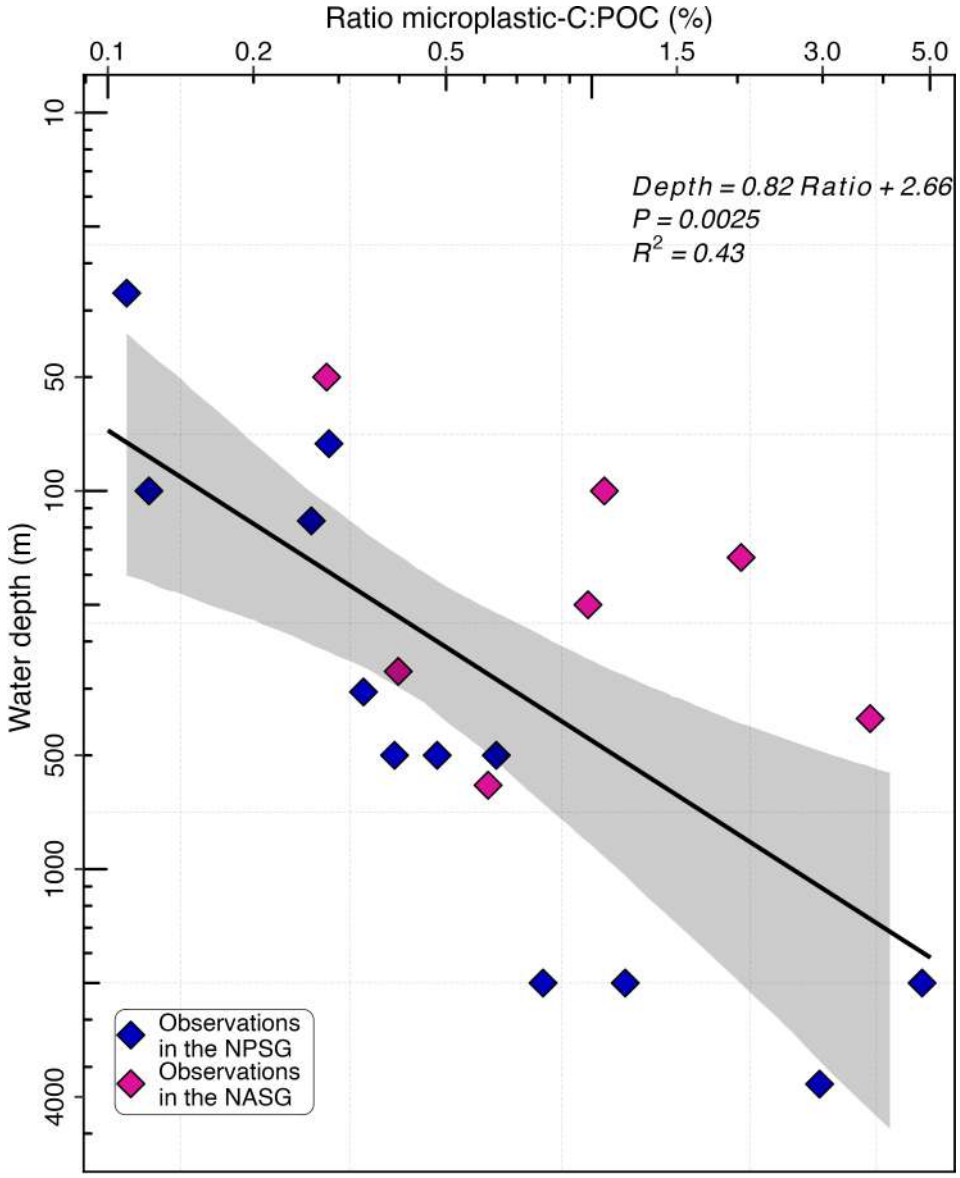

Extended Data Fig. 5 | Relationship between ratios (%) of microplastic-C to particulate organic carbon (POC) and water depth in the North Pacific[25] (blue diamonds) and North Atlantic[22] (purple diamonds) Subtropical Gyres. The black line represents the linear regression fit and the shade area represents the 95% confidence interval estimated by 1000 times of bootstrap.

Extended Data Table 1 | Key methodological steps in studying subsurface microplastics

	Description in the literature	Advantages	Disadvantages
Sampling equipment			
In-situ pump	McLane pump, ISP pump, Plankton pump[a]	-Holding filters of varying pore sizes; -Large sample volume; -Depth resolution (up to 6,000 m); -Ease of controlling contamination	-Selective for small particles; -Labor-intensive and time-consuming operation; -Increased operational challenges during adverse sea states; -High cost
	Submersible pump, Borehole deep-well pump, Ship underway pump	-Ease of operation; -Large sample volume; -Cost-effectiveness; -Ease of controlling contamination	-Limited sampling depth; -Fixed pore/mesh sizes; -Selective for small particles;
Plankton Net	MOCNESS[b], MultNet[c]	-Large sample volume; -Depth resolution[f];	-Labor-intensive and time-consuming operation; -Selective for large particles; -High cost
Bulk water sampler	Niskin bottle, Limnos water sampler, Plexiglass water sampler	-Full depth resolution[g]; -Ease of operation -Ease of controlling contamination	-Limited sample volume
Filter/mesh types			
Screen filter[d]	Anodisc, Polycarbonate filter, Nylon filter, Stainless steel mesh, Cellulose nitrate filter)	-Efficient for capturing larger particles -Easy to wash off the trapped particles	-Limited retention capacity for smaller particles -Prone to clogging
Depth filter[d]	GF/A, GF/C, Quartz filters	- Higher retention capacity for particle of various sizes - handle a relatively high volume of water -Higher resistance to clogging	-Particle are entrapped within the structure
Chemical identification			
Chemical imaging	Single-element mercury cadmium telluride detector, Focal plane array detector	-High spatial resolution (down to 11-20 μm) -Without human bias -Semi-automated data analysis -	-Requiring careful sample preparation -Filter surface sensitivity -Measurement times increasing with imaged filter area -Complexity of analyzing large volume of spectra -Requiring high computational capacity -Instrument expensive
Microscopy-aided inspection following by μ-FTIR/Raman identification	FTIR techniques : Attenuated total reflection-FTIR, μ-FTIR/Raman[e];	-Ease of sample preparation and analysis	-Only applied to particles >100 μm; -Results largely depending on the experience level of the performer
Microscopic inspection	Identifying plastic particles by visual inspection under microscopy	-Ease of large plastic fragments -Low cost	-No polymer information provided

This table outlines the methods used at various stages of subsurface microplastic measurement, including sampling equipment, filter/mesh types, and chemical identification. The advantages and limitations of each step are also provided. [a]The mesh size of plankton pump is fixed. [b]Multiple Opening and Closing net with an Environmental Sensing System. [c]Multiple Plankton Sampler. [d]Screen filter utilizes a mesh screen to physically trap particles larger than the screen openings; Depth filter relies on a porous matrix of depth media to capture particles throughout the depth of the filter medium. [e]μ-FTIR/Raman means microscope-supported spectrometric (Fourier-transform infrared spectroscopy/Raman) systems. [f]MOCNESS and MultiNet can sample at multiple depths, its maximum sampling depth is typically limited compared to in situ pumps. [g]Bulk water sampler (e.g., Niskin bottle CTD Rosette) can allow to collect water samples at precise depths throughout the water column.